**Processed records of the 8 March 2010 Elazığ – Kovancılar, earthquake**

**Earthquake Engineering Research Center**

**Middle East Technical University**

An earthquake occurred on March 8, 2010 at 02:32 (GMT) in the eastern part of Turkey. The epicenter falls in Zone 1 in the Earthquake Zones Map of Turkey. This is the most seismically hazardous zone according to the seismic classification criteria adopted for Turkey (Gülkan et al., 1993). It is located midway between the provincial capital of Elazığ and Bingöl with coordinates reported as 38.7752N-40.0295E by the Earthquake Division of the Turkish Disaster and Emergency Management Agency (DEMA).

The area is sparsely populated, with most dwellings having one or two stories constructed from rubble masonry without timber reinforcement or less frequently, adobe, with thick walls against harsh climate conditions. The roofs of dwellings are inclined corrugated metal with uncut timber serving as the diaphragm. This type of building and its earlier versions topped with a heavy earthen roof have performed very poorly during earthquakes.

The depth and magnitude of the earthquake are reported as 5 km and ML5.8, respectively by the same agency. Other national and international seismic agencies have reported the depth, magnitude, epicentral coordinates as well as other relevant source parameters as listed in Table 1.

Currently a total of 20 three-component accelerometric data is available through the TÜBİTAK[1] funded project entitled "Compilation of National Strong Ground Motion Database in Accordance with International Standards[2]." The data comes from the main and aftershock events. They are acquired by the data automation system established in the Earthquake Division as one of the target objectives in the above project. This first report on the earthquake presents the uniformly processed accelerometric data of these events as well as their Fourier acceleration and response spectra. This information will also be disseminated through the Web at eerc.ce.metu.edu.tr and daphne.deprem.gov.tr. The Web site also contains the raw accelerometric data for researchers who want to do their own data processing. The current document will be updated and expanded regularly and will become a full report after compiling the observations of METU field reconnaissance team that will leave for the area on March 10, 2010. The following pages illustrate the processed waveforms and the calculated spectra for currently available records. Table 2 summarizes the low-cut and high-cut filter cut-offs determined by the procedure described in Akkar and Bommer (2006). The same table also lists the suggested usable period ranges of each recording based on the empirical expressions derived in the same article. The processing and spectral calculations are done by using the USDP software that is developed within the context of the above project.

References:

Akkar, S. and Bommer J.J., 2006. " Influence of long-period filter cut-off on elastic spectral displacements," *Earthquake Engineering and Structural Dynamics* , 35(9), 1145-1165.

Gulkan P., Koçyiğit A., Yücemen M.S., Doyuran V. and Başöz N. (1993). "Turkish seismic zonation map prepared by the most recent earthquake data," Report No. 93-01, Earthquake Engineering Research Center, Middle East Technical University 06531, Ankara Turkey.

---

[1] Scientific and Technological Research Council of Turkey
[2] This project is jointly launched by the Earthquake Department of the Disaster and Emergency Management State Agency and the Earthquake Engineering Research Center of Middle East Technical University.

Acknowledgments:

Contributors:

Abdullah Sandıkkaya
Emrah Yenier
Sinan Akkar

Table 1. Important seismological features of the main and aftershock earthquakes reported by national and international seismological agencies

| Agency | Date | Time (GMT) | Epicenter Latitude | Epicenter Longitude | Depth (km) | $M_w$ | $M_b$ | $M_s$ | $M_L$ | $M_0$ (dyne.cm) |
|---|---|---|---|---|---|---|---|---|---|---|
| DEMA[3] | 08-03-10 | 02:32:30 | 38.7752 | 40.0295 | 5.0 | - | - | - | 5.8 | - |
| KOERI[4] | 08-03-10 | 02:32:31 | 38.807 | 40.0998 | 5.0 | - | - | - | 6.0 | - |
| GCMT[5] | 08-03-10 | 02:32:39 | 38.89 | 40.02 | 15.6 | 6.1 | 5.9 | 5.9 | - | 1.55E+25 |
| RCMT[6] | 08-03-10 | 02:32:40 | 38.95 | 40.00 | 15.0 | 6.1 | - | - | - | 1.60E+25 |
| USGS[7] | 08-03-10 | 02:32:36 | 38.888 | 40.022 | 21.0 | 6.0 | - | - | - | 1.40E+25 |

| Agency | T-axes PLG | T-axes AZ | N-axes PLG | N-axes AZ | P-axes PLG | P-axes AZ | 1st Plane Strike | 1st Plane Dip | 1st Plane Slip | 2nd Plane Strike | 2nd Plane Dip | 2nd Plane Slip | Correct Plane |
|---|---|---|---|---|---|---|---|---|---|---|---|---|---|
| DEMA | - | - | - | - | - | - | - | - | - | - | - | - | - |
| KOERI | - | - | - | - | - | - | - | - | - | - | - | - | - |
| GCMT | - | - | - | - | - | - | 320 | 66 | -174 | 228 | 85 | 24 | 2 |
| RCMT | 15 | 275 | 67 | 46 | 16 | 181 | 318 | 67 | -179 | 228 | 89 | -23 | 2 |
| USGS | 4 | 272 | 77 | 22 | 11 | 181 | 227 | 85 | -11 | 318 | 79 | -174 | 1 |

[3] Earthquake Department of the Disaster and Emergency Management State Agency (abbreviated as State Earthquake Department in this document).
[4] Kandilli Observatory and Earthquake Research Institute
[5] Global Centroid Moment Tensor
[6] European Mediterranean Regional Centroid Moment Tensors Database
[7] United States Geological Survey

Table 1 (continued)

| Agency | Date | Time (GMT) | Epicenter Latitude | Epicenter Longitude | Depth (km) | $M_w$ | $M_b$ | $M_s$ | $M_L$ | $M_0$ (dyne.cm) |
|---|---|---|---|---|---|---|---|---|---|---|
| DEMA | 08/03/10 | 07:47:37 | 38.7355 | 40.009 | 5.0 | - | - | - | 5.6 | - |
| KOERI | 08/03/10 | 07:47:38 | 38.7805 | 40.066 | 5.0 | - | - | - | 5.5 | - |
| GCMT | 08/03/10 | 07:47:44 | 38.81 | 39.96 | 15.2 | 5.6 | 5.5 | 5.5 | - | 2.78E+24 |
| RCMT | 08/03/10 | 07:47:44 | 38.77 | 40 | 17.0 | 5.6 | - | - | - | 3.00E+24 |
| USGS | 08/03/10 | 02:32:30 | - | - | - | - | - | - | - | - |

| Agency | T-axes PLG | T-axes AZ | N-axes PLG | N-axes AZ | P-axes PLG | P-axes AZ | 1st Plane Strike | 1st Plane Dip | 1st Plane Slip | 2nd Plane Strike | 2nd Plane Dip | 2nd Plane Slip | Correct Plane |
|---|---|---|---|---|---|---|---|---|---|---|---|---|---|
| DEMA | - | - | - | - | - | - | - | - | - | - | - | - | - |
| KOERI | - | - | - | - | - | - | - | - | - | - | - | - | - |
| GCMT | - | - | - | - | - | - | 322 | 81 | -171 | 230 | 81 | -9 | 2 |
| RCMT | 1 | 276 | 70 | 7 | 20 | 185 | 322 | 75 | -166 | 229 | 76 | -15 | 2 |
| USGS | - | - | - | - | - | - | - | - | - | - | - | - | - |

Table 1 (continued)

| Agency | Date | Time (GMT) | Epicenter Latitude | Epicenter Longitude | Depth (km) | $M_L$ |
|--------|------|------------|--------------------|--------------------|-----------|-------|
| DEMA | 08/03/10 | 03:20:22 | 38.7948 | 40.0705 | 5.0 | 4.4 |
| KOERI | 08/03/10 | 03:20:22 | 38.8698 | 40.2325 | 5.0 | 4.1 |

| Agency | Date | Time (GMT) | Epicenter Latitude | Epicenter Longitude | Depth (km) | $M_L$ |
|--------|------|------------|--------------------|--------------------|-----------|-------|
| DEMA | 08/03/10 | 08:11:20 | 38.7412 | 40.0138 | 10.0 | 4.2 |
| KOERI | 08/03/10 | 08:11:20 | 38.7357 | 40.076 | 5.1 | 4.3 |

| Agency | Date | Time (GMT) | Epicenter Latitude | Epicenter Longitude | Depth (km) | $M_L$ |
|--------|------|------------|--------------------|--------------------|-----------|-------|
| DEMA | 08/03/10 | 09:00:46 | 38.7468 | 40.006 | 4.1 | 4.8 |
| KOERI | 08/03/10 | 09:00:46 | 38.761 | 40.0615 | 5.0 | 4.8 |

| Agency | Date | Time (GMT) | Epicenter Latitude | Epicenter Longitude | Depth (km) | $M_L$ |
|--------|------|------------|--------------------|--------------------|-----------|-------|
| DEMA | 08/03/10 | 10:14:23 | 38.7685 | 40.0772 | 7.7 | 5.0 |
| KOERI | 08/03/10 | 10:14:23 | 38.828 | 40.1187 | 5.0 | 5.1 |

Table 2. Important properties of the processed records from the main and aftershock events

| Record Names | Instrument Type | Record Information | $f_{lc}$-NS | $f_{hc}$-NS | Usable period-NS | $f_{lc}$-EW | $f_{hc}$-EW | Usable period-EW | $f_{lc}$-UD | $f_{hc}$-UD | Usable period-UD |
|---|---|---|---|---|---|---|---|---|---|---|---|
| 20100308023229_0201 | CMG-5TD | | 0.100 | 25 | 9.0 | 0.075 | 25 | 12.0 | 0.050 | 30 | 18.0 |
| 20100308023229_1201 | CMG-5TD | | 0.050 | 40 | 18.0 | 0.075 | 40 | 12.0 | 0.050 | 40 | 18.0 |
| 20100308023229_1206 | CMG-5TD | | 0.050 | 35 | 19.4 | 0.050 | 35 | 19.4 | 0.075 | 40 | 12.9 |
| 20100308023229_2101 | CMG-5TD | | 0.100 | 30 | 9.0 | 0.050 | 30 | 18.0 | 0.100 | 30 | 9.0 |
| 20100308023229_2301 | CMG-5TD | | 0.075 | 30 | 12.0 | 0.100 | 30 | 9.0 | 0.050 | 40 | 18.0 |
| 20100308023229_2303 | SM-2 | | 0.075 | 20 | 12.9 | 0.075 | 20 | 12.9 | 0.100 | 25 | 9.7 |
| 20100308023229_4701 | CMG-5TD | | 0.100 | 35 | 9.0 | 0.100 | 35 | 9.0 | 0.075 | 30 | 12.0 |
| 20100308023229_7201 | CMG-5TD | | 0.050 | 35 | - | 0.075 | 30 | - | 0.100 | 35 | - |
| 20100308032022_2303 | SM-2 | IDR | - | - | - | - | - | - | - | - | - |
| 20100308074737_1201 | CMG-5TD | | 0.100 | 30 | 9.0 | 0.075 | 30 | 12.0 | 0.075 | 40 | 12.0 |
| 20100308074737_1206 | CMG-5TD | | 0.075 | 25 | 12.9 | 0.075 | 30 | 12.9 | 0.075 | 30 | 12.9 |
| 20100308074737_2301 | CMG-5TD | | 0.075 | 30 | 12.0 | 0.075 | 30 | 12.0 | 0.100 | 30 | 9.0 |
| 20100308074737_2303 | SM-2 | | 0.100 | 25 | 9.7 | 0.100 | 20 | 9.7 | 0.100 | 35 | 9.7 |
| 20100308081120_2303 | SM-2 | | 0.100 | 20 | 9.7 | 0.150 | 20 | 6.5 | 0.200 | 30 | 4.9 |
| 20100308090046_1201 | CMG-5TD | | 0.100 | 25 | 9.0 | 0.150 | 25 | 6.0 | 0.150 | 30 | 6.0 |
| 20100308090046_2303 | SM-2 | | 0.100 | 20 | 9.7 | 0.150 | 20 | 6.5 | 0.150 | 25 | 6.5 |
| 20100308101423_1201 | CMG-5TD | | 0.050 | 40 | 18.0 | 0.100 | 40 | 9.0 | 0.150 | 40 | 6.0 |
| 20100308101423_1206 | CMG-5TD | | 0.100 | 40 | 9.7 | 0.100 | 40 | 9.7 | 0.100 | 40 | 9.7 |
| 20100308101423_2303 | SM-2 | | 0.150 | 15 | 6.5 | 0.150 | 20 | 6.5 | 0.200 | 25 | 4.9 |
| 20100308XXXXXX_2303 | SM-2 | IDR | - | - | - | - | - | - | - | - | - |

$f_{lc}$: Low-cut filter frequency
$f_{hc}$: High-cut filter frequency
IDR: Insufficient digitizer resolution

Table 2 (continued)

| Record Names | Processed PGA_NS (cm/s$^2$) | Processed PGA_EW (cm/s$^2$) | Processed PGA_UD (cm/s$^2$) | Processed PGV_NS (cm/s) | Processed PGV_EW (cm/s) | Processed PGV_UD (cm/s) |
|---|---|---|---|---|---|---|
| 20100308023229_0201 | 2.43 | 2.23 | 1.65 | 0.95 | 0.75 | 0.38 |
| 20100308023229_1201 | 55.43 | 34.27 | 25.50 | 5.10 | 3.78 | 1.74 |
| 20100308023229_1206 | 11.59 | 17.84 | 8.95 | 1.96 | 1.23 | 0.99 |
| 20100308023229_2101 | 3.44 | 5.10 | 2.60 | 0.52 | 0.68 | 0.35 |
| 20100308023229_2301 | 5.56 | 4.76 | 3.85 | 1.01 | 0.71 | 0.48 |
| 20100308023229_2303 | 62.14 | 66.59 | 30.04 | 7.30 | 5.99 | 3.24 |
| 20100308023229_4701 | 2.56 | 2.48 | 1.68 | 0.35 | 0.50 | 0.18 |
| 20100308023229_7201 | 7.61 | 5.42 | 2.52 | 1.27 | 1.09 | 0.27 |
| 20100308032022_2303 | - | - | - | - | - | - |
| 20100308074737_1201 | 14.54 | 10.21 | 7.07 | 1.10 | 0.83 | 0.55 |
| 20100308074737_1206 | 2.81 | 3.85 | 1.54 | 0.31 | 0.34 | 0.17 |
| 20100308074737_2301 | 3.54 | 4.22 | 3.33 | 0.60 | 0.50 | 0.45 |
| 20100308074737_2303 | 76.26 | 47.79 | 55.01 | 10.37 | 3.85 | 4.38 |
| 20100308081120_2303 | 7.78 | 6.86 | 4.98 | 0.56 | 0.58 | 0.36 |
| 20100308090046_1201 | 2.72 | 3.01 | 2.43 | 0.17 | 0.14 | 0.12 |
| 20100308090046_2303 | 15.50 | 12.95 | 9.18 | 1.68 | 0.95 | 0.78 |
| 20100308101423_1201 | 8.67 | 8.12 | 5.31 | 0.44 | 0.47 | 0.24 |
| 20100308101423_1206 | 2.25 | 2.21 | 1.48 | 0.17 | 0.17 | 0.08 |
| 20100308101423_2303 | 16.42 | 13.42 | 11.10 | 1.38 | 0.96 | 1.00 |
| 20100308XXXXXX_2303 | - | - | - | - | - | - |

PGA: Peak ground acceleration
PGV: Peak ground velocity

Table 2 (continued)

| Record Names | Station Code | Station Latitude | Station Longitude | $V_{S30}$ | $R_{epi}$ DEMA (km) | $R_{hyp}$ DEMA (km) | $R_{epi}$ KOERI (km) | $R_{hyp}$ KOERI (km) |
|---|---|---|---|---|---|---|---|---|
| 20100308023229_0201 | 0201 | 37.76121 | 38.26742 | 391 | 190.9 | 190.9 | 197.9 | 197.9 |
| 20100308023229_1201 | 1201 | 38.89708 | 40.5032 | 529 | 43.3 | 43.6 | 36.4 | 36.8 |
| 20100308023229_1206 | 1206 | 39.29345 | 41.00883 | 356 | 102.4 | 102.6 | 95.4 | 95.5 |
| 20100308023229_2101 | 2101 | 37.93088 | 40.20278 | 519 | 94.9 | 95.0 | 97.6 | 97.8 |
| 20100308023229_2301 | 2301 | 38.67043 | 39.19267 | 407 | 73.7 | 73.8 | 80.3 | 80.4 |
| 20100308023229_2303 | 2303 | 38.69577 | 39.9319 | 329 | 12.2 | 13.2 | 19.1 | 19.8 |
| 20100308023229_4701 | 4701 | 37.32632 | 40.72374 | 709 | 172.0 | 172.0 | 173.2 | 173.3 |
| 20100308023229_7201 | 7201 | 37.873 | 41.15112 | | 140.1 | 140.2 | 138.5 | 138.6 |
| 20100308032022_2303 | 2303 | 38.69577 | 39.9319 | 329 | 16.3 | 17.1 | 32.5 | 32.9 |
| 20100308074737_1201 | 1201 | 38.89708 | 40.5032 | 529 | 46.5 | 46.8 | 40.1 | 40.4 |
| 20100308074737_1206 | 1206 | 39.29345 | 41.00883 | 356 | 106.4 | 106.6 | 99.5 | 99.6 |
| 20100308074737_2301 | 2301 | 38.67043 | 39.19267 | 407 | 71.4 | 71.5 | 76.9 | 77.1 |
| 20100308074737_2303 | 2303 | 38.69577 | 39.9319 | 329 | 8.0 | 9.5 | 15.0 | 15.8 |
| 20100308081120_2303 | 2303 | 38.69577 | 39.9319 | 329 | 8.7 | 13.3 | 13.3 | 14.2 |
| 20100308090046_1201 | 1201 | 38.89708 | 40.5032 | 529 | 46.3 | 46.5 | 41.2 | 41.5 |
| 20100308090046_2303 | 2303 | 38.69577 | 39.9319 | 329 | 8.6 | 9.5 | 13.4 | 14.3 |
| 20100308101423_1201 | 1201 | 38.89708 | 40.5032 | 529 | 39.6 | 40.4 | 34.2 | 34.6 |
| 20100308101423_1206 | 1206 | 39.29345 | 41.00883 | 356 | 99.5 | 99.8 | 92.7 | 92.9 |
| 20100308101423_2303 | 2303 | 38.69577 | 39.9319 | 329 | 15.0 | 16.8 | 21.9 | 22.4 |
| 20100308XXXXXX_2303 | 2303 | 38.69577 | 39.9319 | 329 | - | - | - | - |

$V_{S30}$: The mean S-wave velocity of the top 30m of the soil profile
$R_{epi}$: Epicentral distance
$R_{hyp}$: Hypocentral distance

Table 2 (continued)

| Record Names | Station Code | R_epi GCMT (km) | R_hyp GCMT (km) | R_JB GCMT (km) | R_rup GCMT (km) | R_epi RCMT (km) | R_hyp RCMT (km) | R_JB RCMT (km) | R_rup RCMT (km) | R_epi USGS (km) | R_hyp USGS (km) | R_JB USGS (km) | R_rup USGS (km) |
|---|---|---|---|---|---|---|---|---|---|---|---|---|---|
| 20100308023229_0201 | 0201 | 197.9 | 198.5 | 190.7 | 191.0 | 200.8 | 201.4 | 193.6 | 193.9 | 197.9 | 199.0 | 191.6 | 192.4 |
| 20100308023229_1201 | 1201 | 41.9 | 44.7 | 36.3 | 38.0 | 44.0 | 46.5 | 39.4 | 40.8 | 41.8 | 46.7 | 36.8 | 40.5 |
| 20100308023229_1206 | 1206 | 96.5 | 97.8 | 89.4 | 90.1 | 95.2 | 96.4 | 88.2 | 88.9 | 96.5 | 98.7 | 90.3 | 91.8 |
| 20100308023229_2101 | 2101 | 107.6 | 108.8 | 103.8 | 104.4 | 114.5 | 115.5 | 110.9 | 111.4 | 107.4 | 109.4 | 103.9 | 105.3 |
| 20100308023229_2301 | 2301 | 75.9 | 77.5 | 69.1 | 70.3 | 76.7 | 78.1 | 69.7 | 70.6 | 76.0 | 78.8 | 70.1 | 72.4 |
| 20100308023229_2303 | 2303 | 22.9 | 27.7 | 16.8 | 20.2 | 28.8 | 32.5 | 23.6 | 25.9 | 22.7 | 30.9 | 17.3 | 24.2 |
| 20100308023229_4701 | 4701 | 184.2 | 184.8 | 181.5 | 181.9 | 191.0 | 191.6 | 188.6 | 188.9 | 183.9 | 185.1 | 181.4 | 182.2 |
| 20100308023229_7201 | 7201 | 150.0 | 150.8 | 149.5 | 149.9 | 156.2 | 156.9 | 156.1 | 156.4 | 149.7 | 151.2 | 149.3 | 150.3 |
| 20100308032022_2303 | 2303 | - | - | - | - | - | - | - | - | - | - | - | - |
| 20100308074737_1201 | 1201 | 48.1 | 50.5 | 44.6 | 46.3 | 45.9 | 49.0 | 42.2 | 44.5 | - | - | - | - |
| 20100308074737_1206 | 1206 | 105.4 | 106.5 | 101.8 | 102.5 | 104.9 | 106.3 | 101.2 | 102.2 | - | - | - | - |
| 20100308074737_2301 | 2301 | 68.5 | 70.1 | 65.0 | 66.5 | 71.1 | 73.1 | 67.5 | 69.7 | - | - | - | - |
| 20100308074737_2303 | 2303 | 12.9 | 19.9 | 10.1 | 15.8 | 10.1 | 19.8 | 6.4 | 15.5 | - | - | - | - |
| 20100308081120_2303 | 2303 | - | - | - | - | - | - | - | - | - | - | - | - |
| 20100308090046_1201 | 1201 | - | - | - | - | - | - | - | - | - | - | - | - |
| 20100308090046_2303 | 2303 | - | - | - | - | - | - | - | - | - | - | - | - |
| 20100308101423_1201 | 1201 | - | - | - | - | - | - | - | - | - | - | - | - |
| 20100308101423_1206 | 1206 | - | - | - | - | - | - | - | - | - | - | - | - |
| 20100308101423_2303 | 2303 | - | - | - | - | - | - | - | - | - | - | - | - |
| 20100308XXXXXX_2303 | 2303 | - | - | - | - | - | - | - | - | - | - | - | - |

$R_{JB}$: Joyner-Boore distance (the closest distance from site to the vertical projection of the rupture plane)
$R_{rup}$: Rupture distance (the closest distance from site to the rupture plane)

Figure 1. Epicenter of the mainshock and national strong-motion stations that recorded the mainshock (from Google Earth)

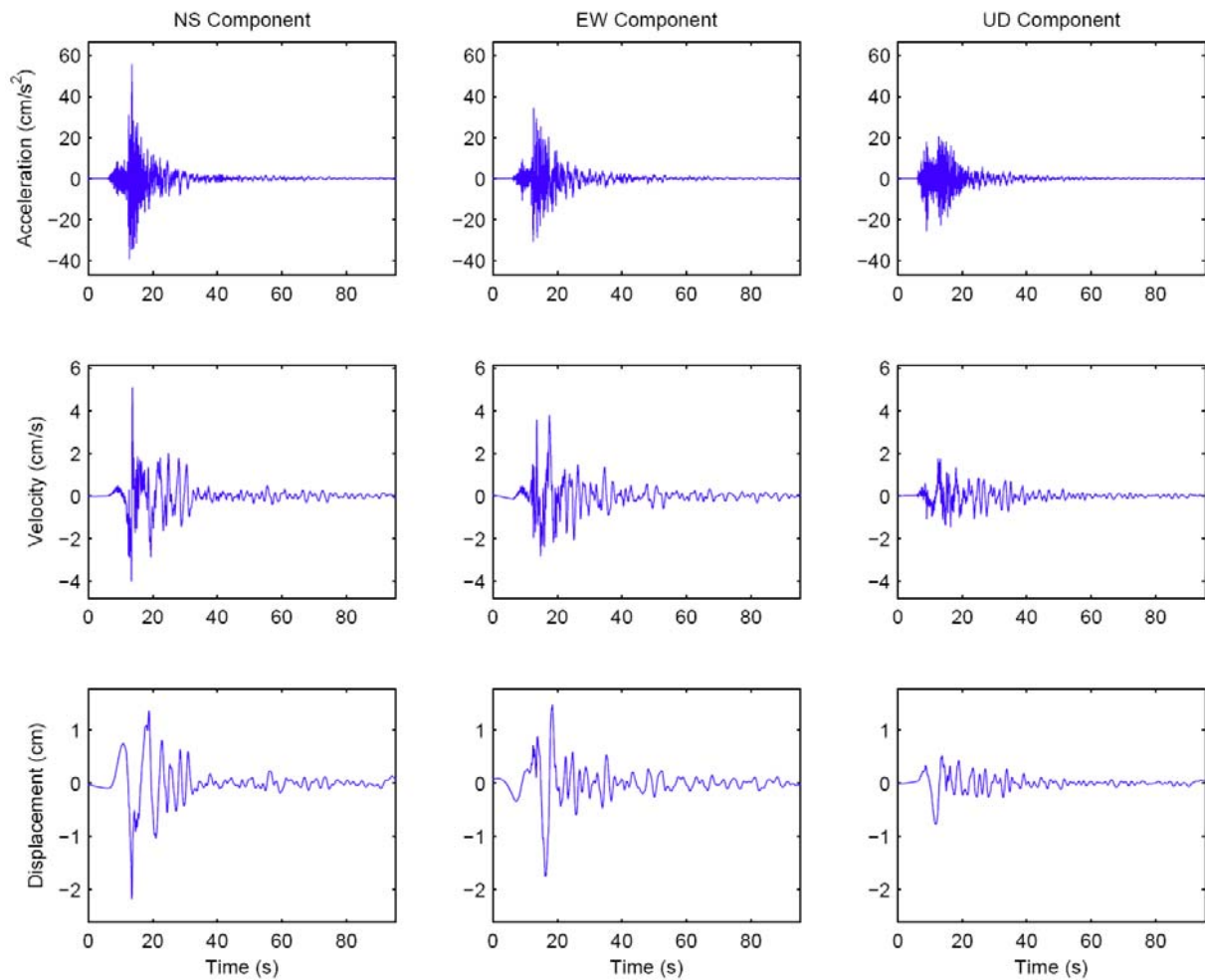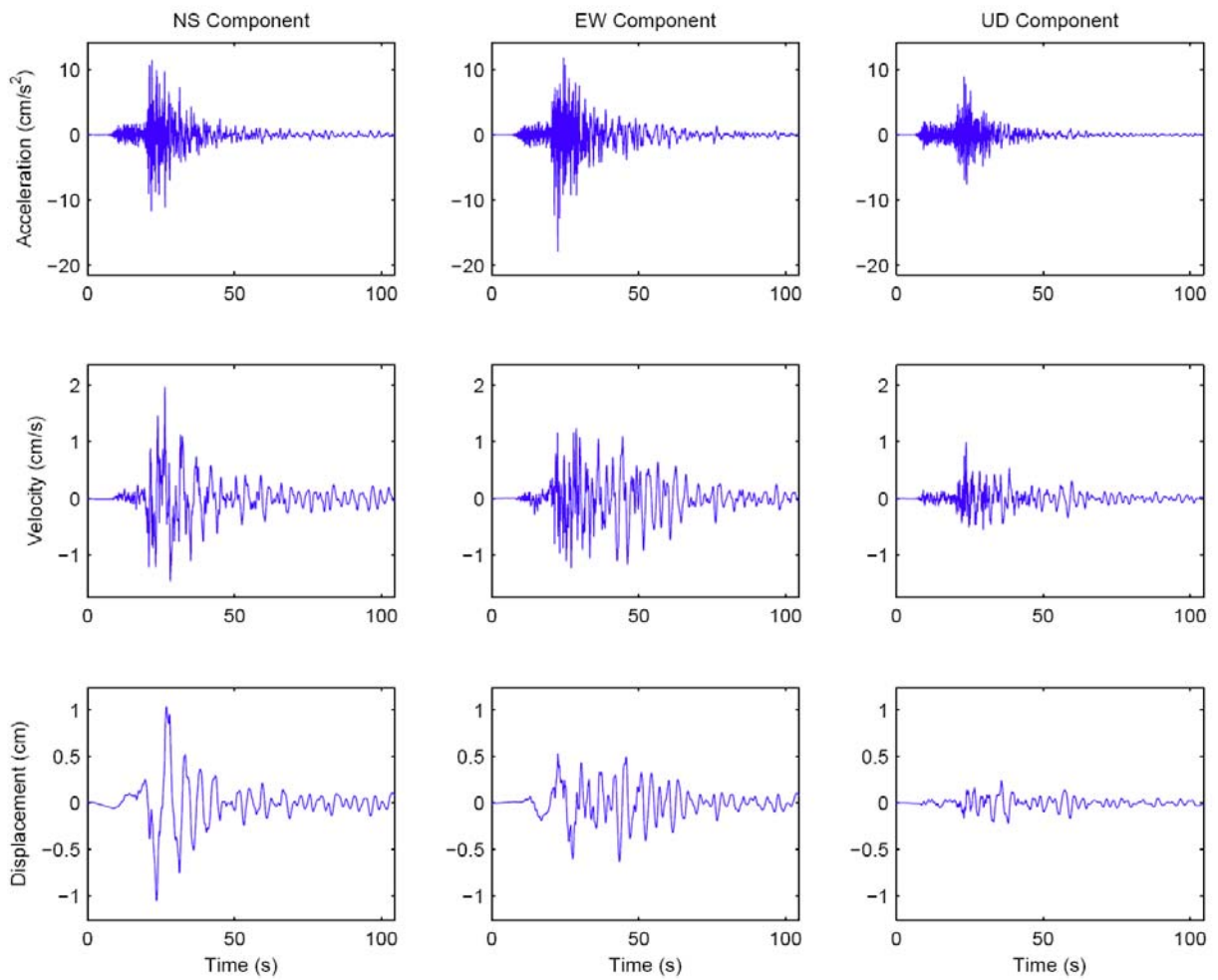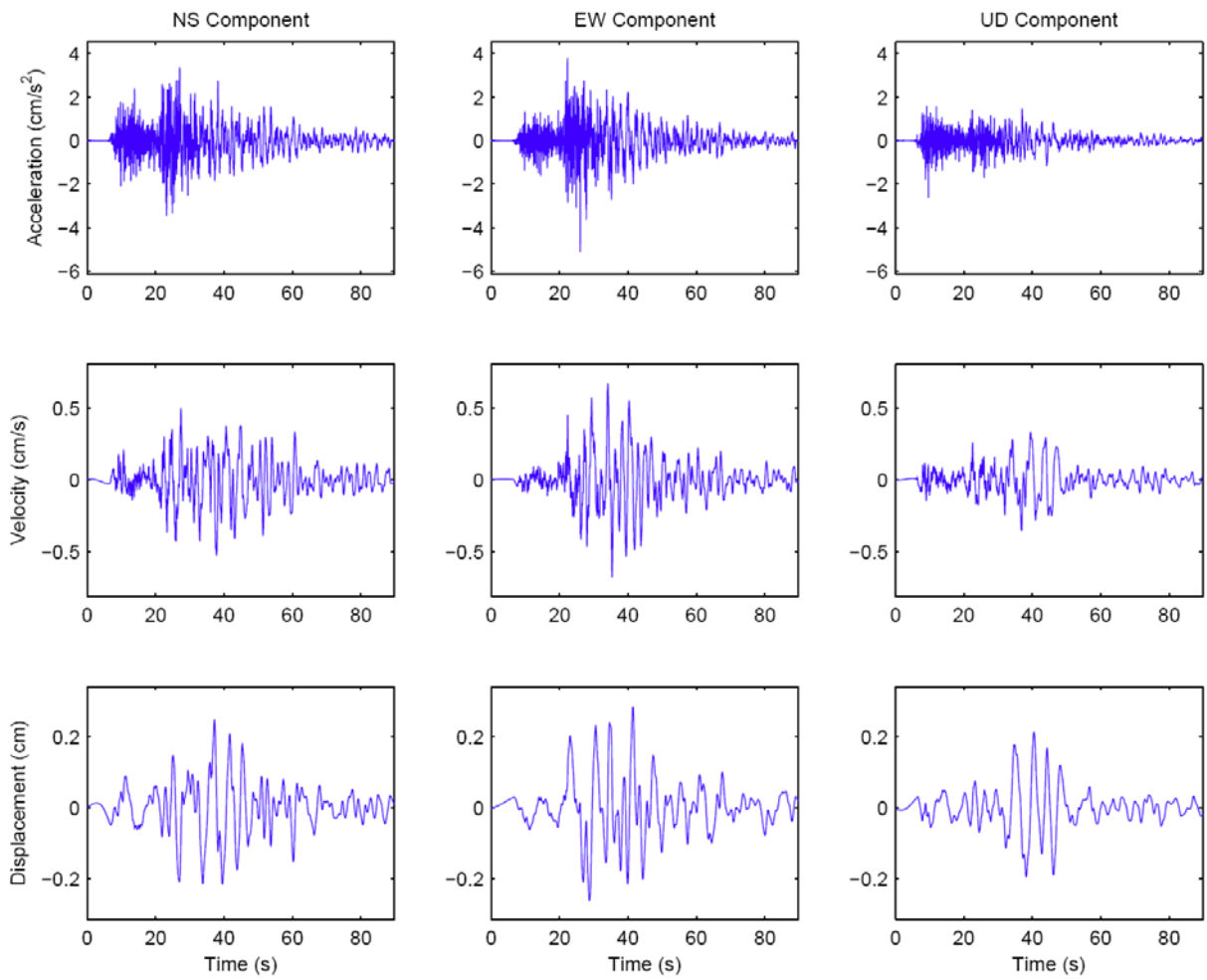**Ground Motions of the 08/03/2010 02:32:29 Elazığ-Kovancılar, Earthquake**
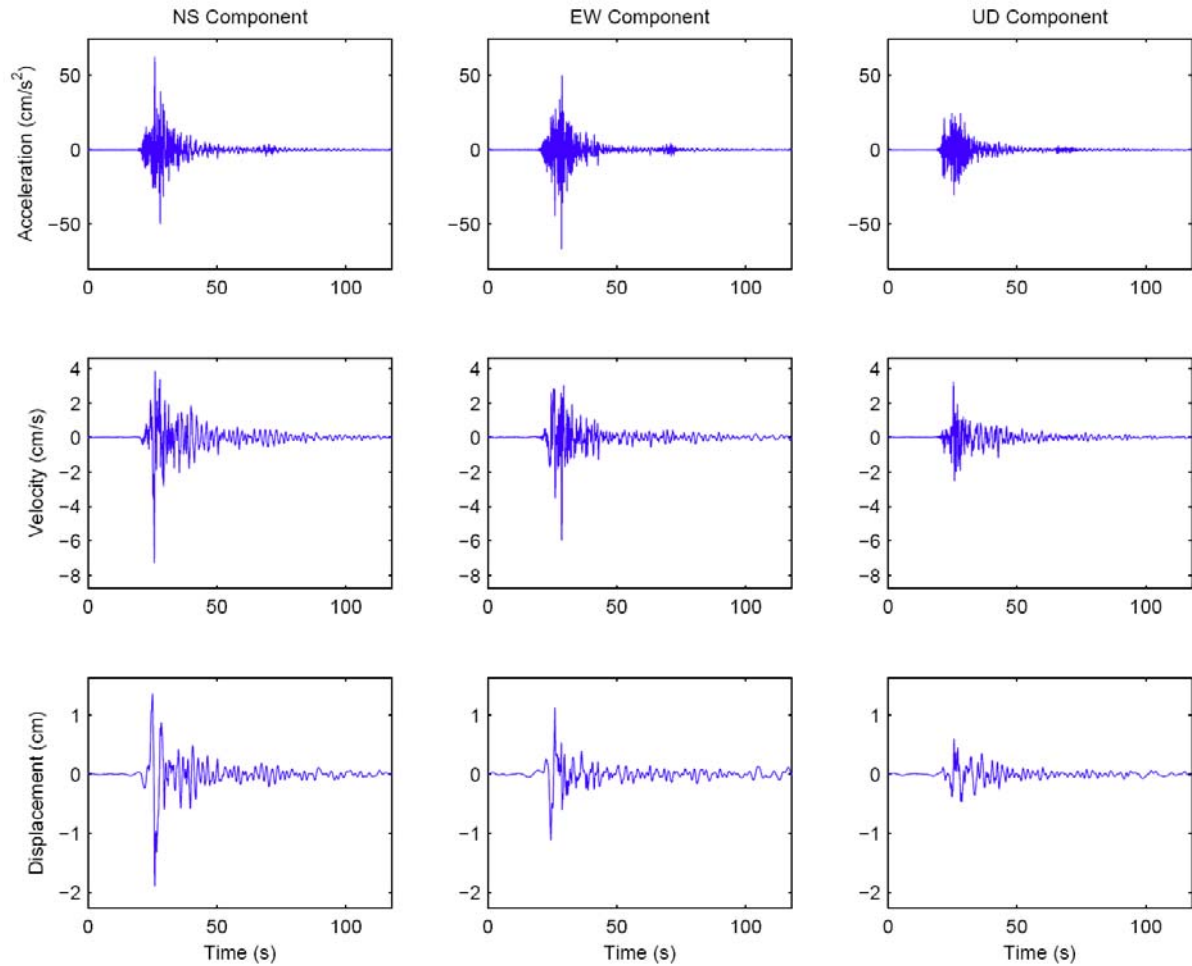


Figure 2. Acceleration (top row), velocity (middle row) and displacement (bottom row) time series of the processed ground motions recorded at Elazığ-Palu (Record Name: 20100308023229_2303, Station Code: 2303). The waveforms are band-pass filtered by acausal 4-pole/4-pole Butterworth filter. Zero pads due to acausal filter transients are not shown for illustrative purposes.
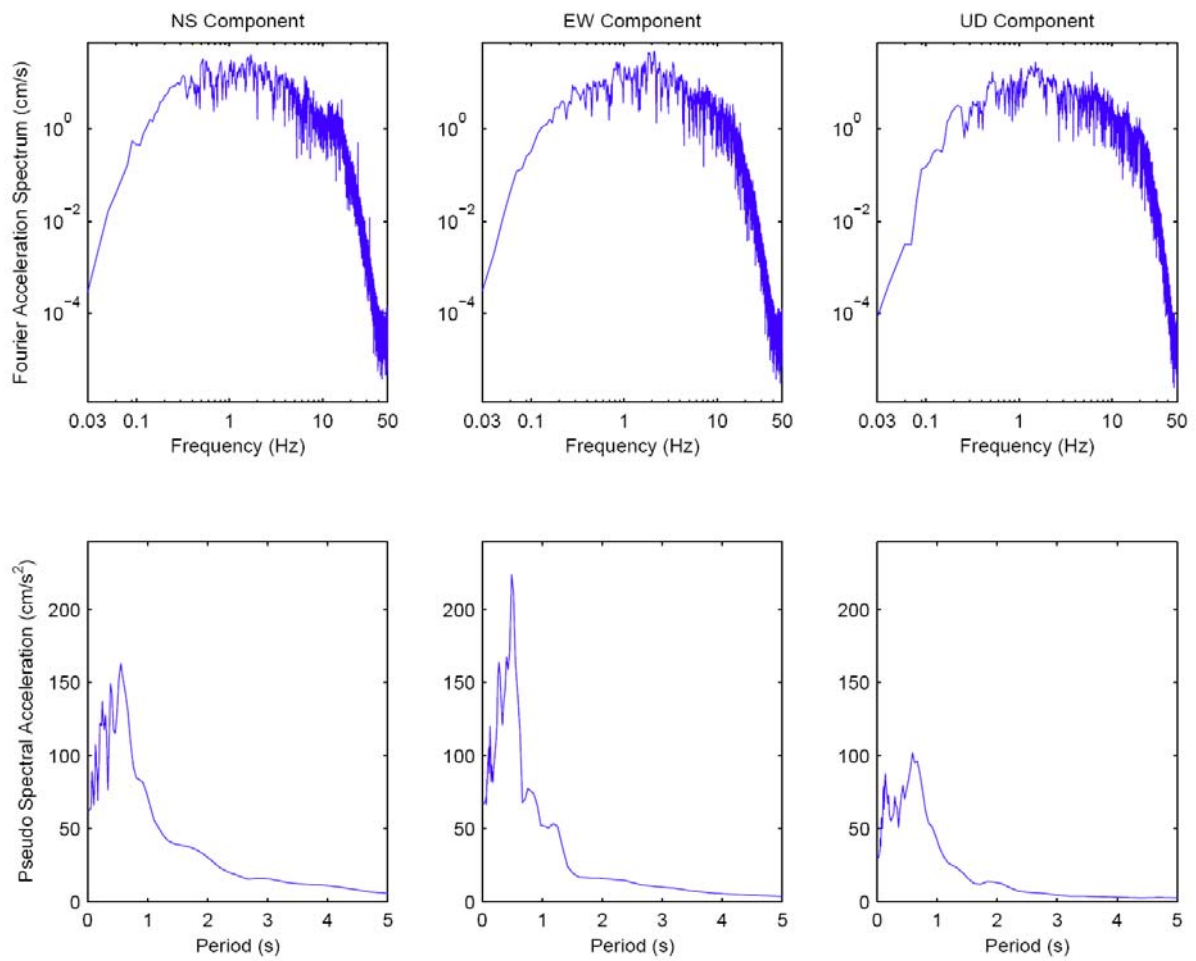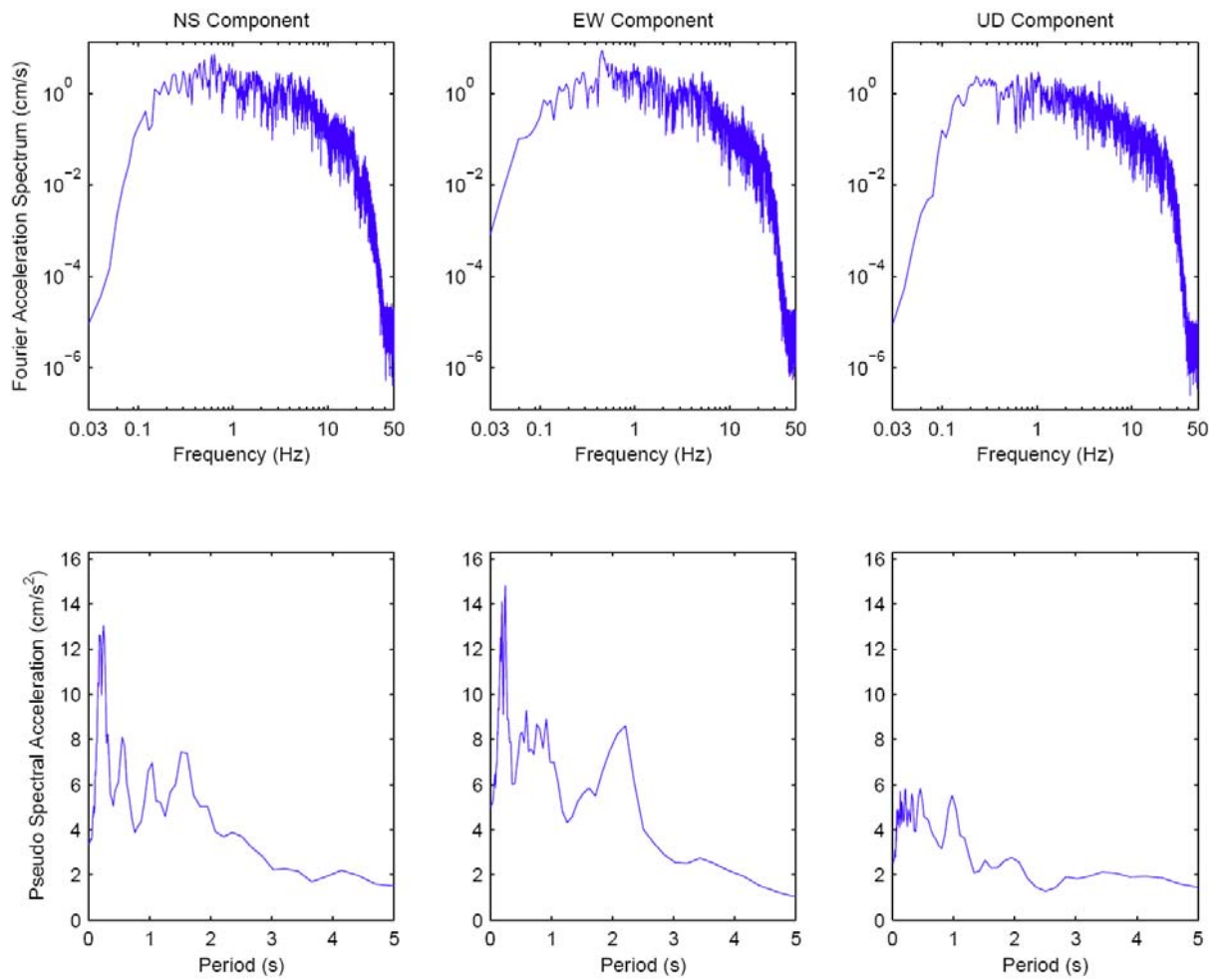
Figure 3. Fourier acceleration spectra (top row) and 5-percent damped pseudo-spectral accelerations (bottom row) of the processed ground motions recorded at Elazığ-Palu (Record Name: 20100308023229_2303, Station Code: 2303).
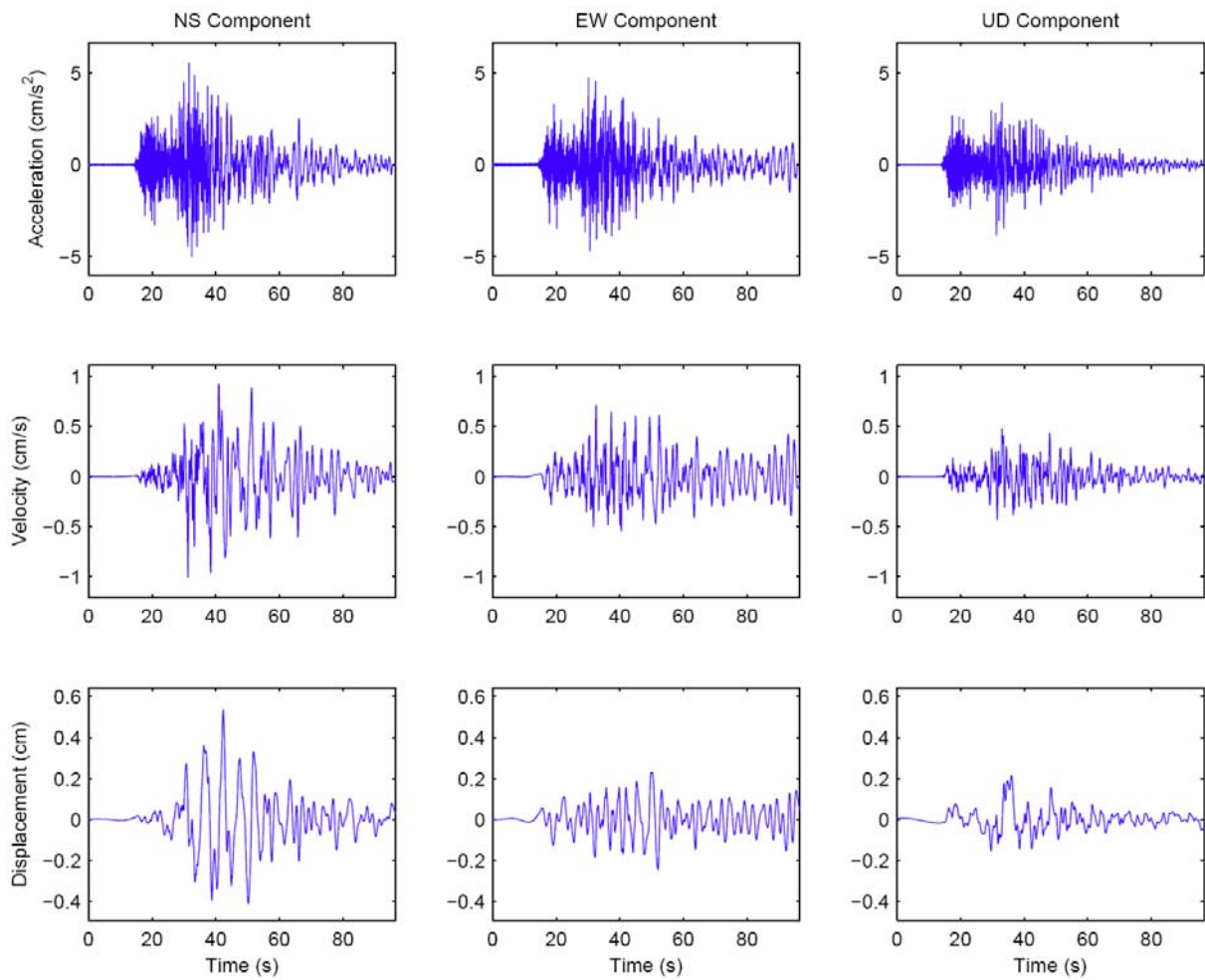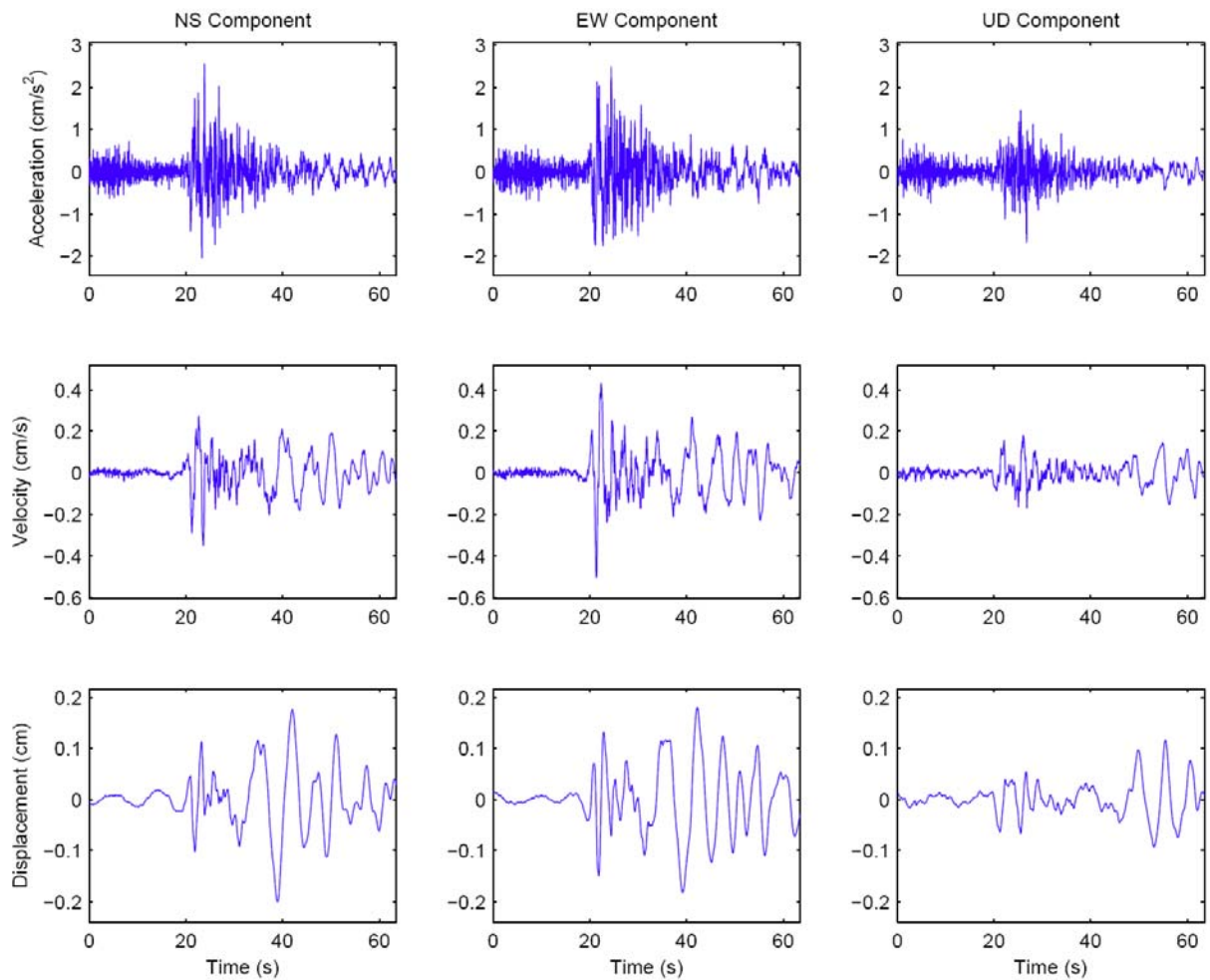
Figure 4. Acceleration (top row), velocity (middle row) and displacement (bottom row) time series of the processed ground motions recorded at Elazığ-Merkez (Record Name: 20100308023229_2301, Station Code: 2301). The waveforms are band-pass filtered by acausal 4-pole/4-pole Butterworth filter. Zero pads due to acausal filter transients are not shown for illustrative purposes.
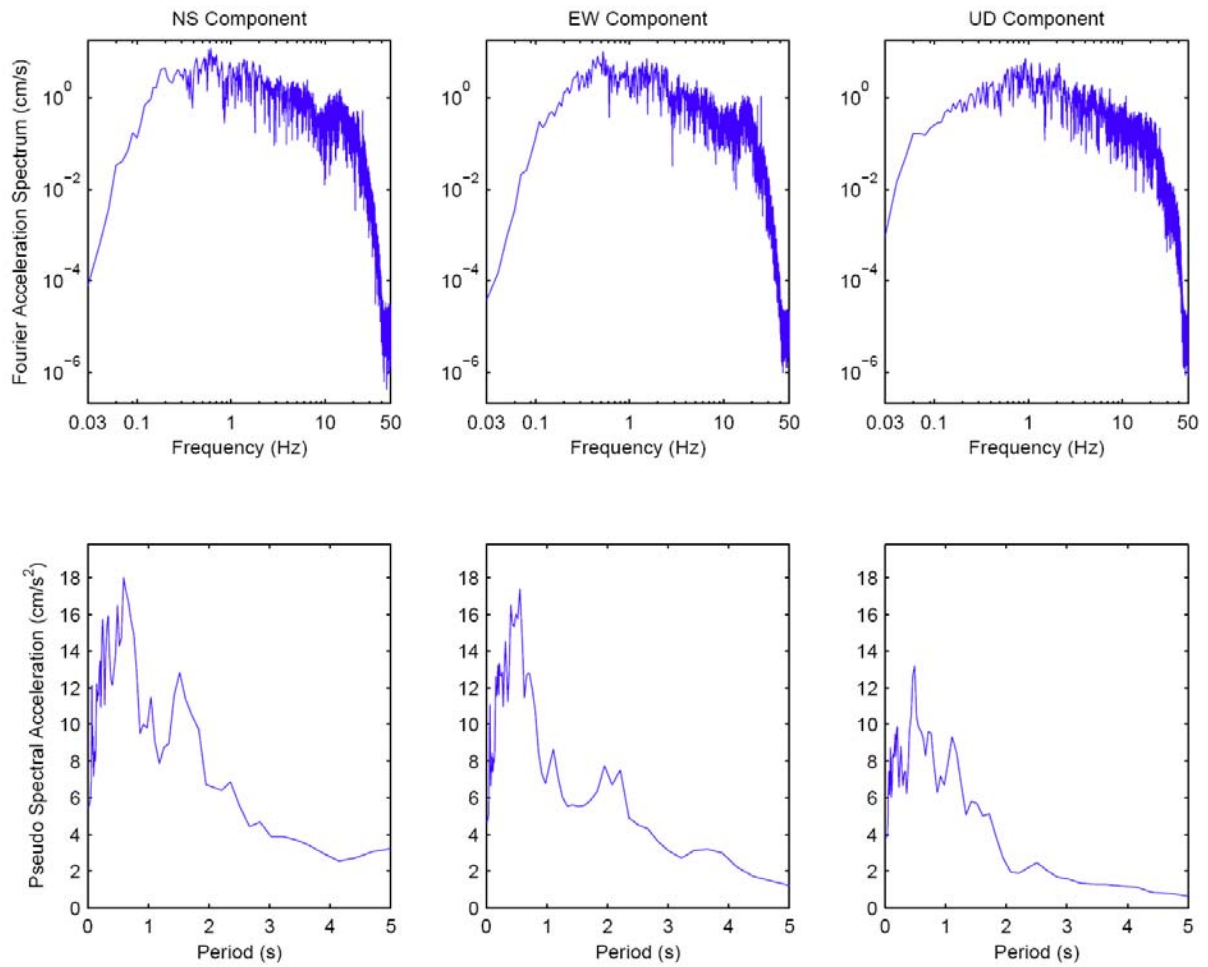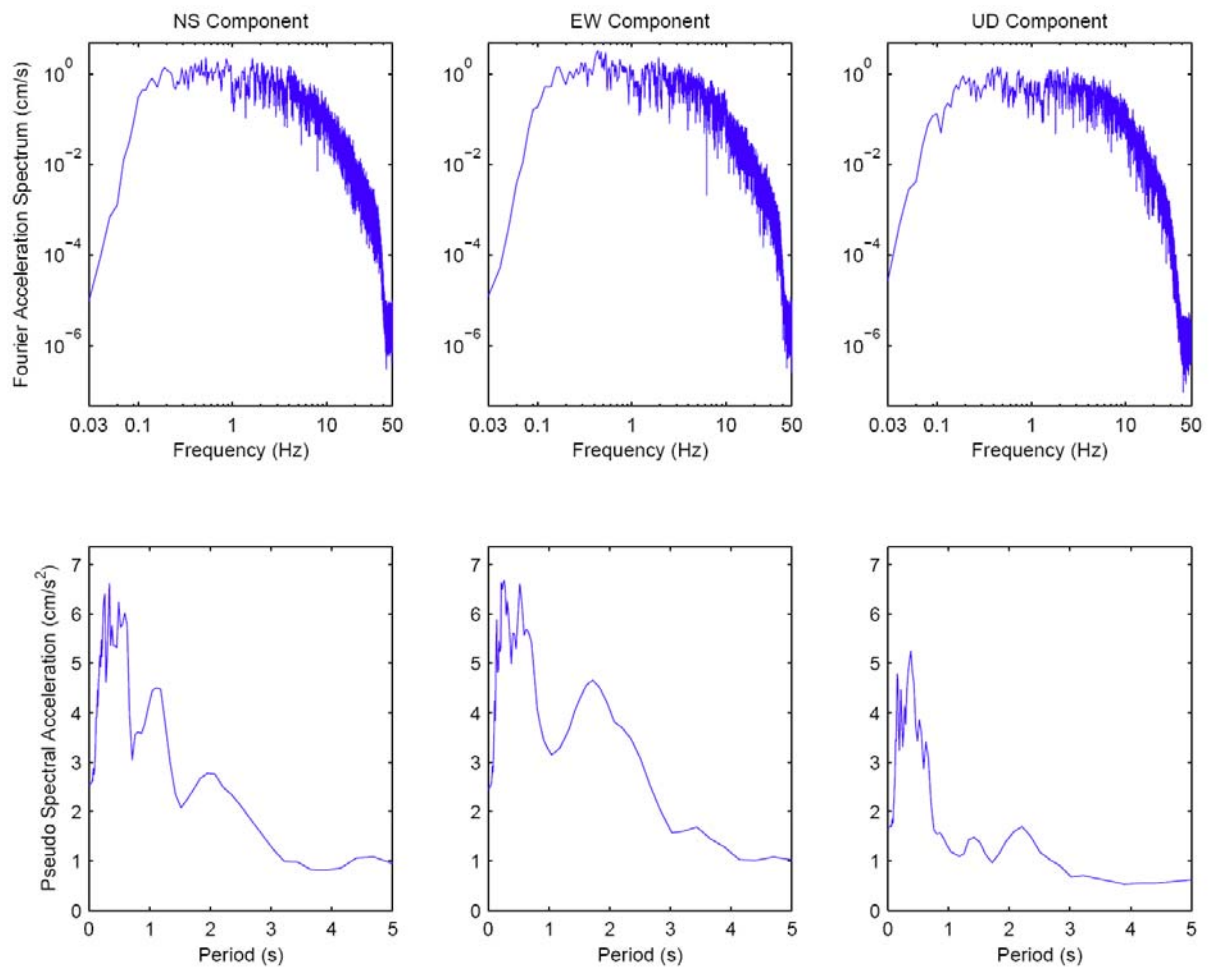
Figure 5. Fourier acceleration spectra (top row) and 5-percent damped pseudo-spectral accelerations (bottom row) of the processed ground motions recorded at Elazığ-Merkez (Record Name: 20100308023229_2301, Station Code: 2301).
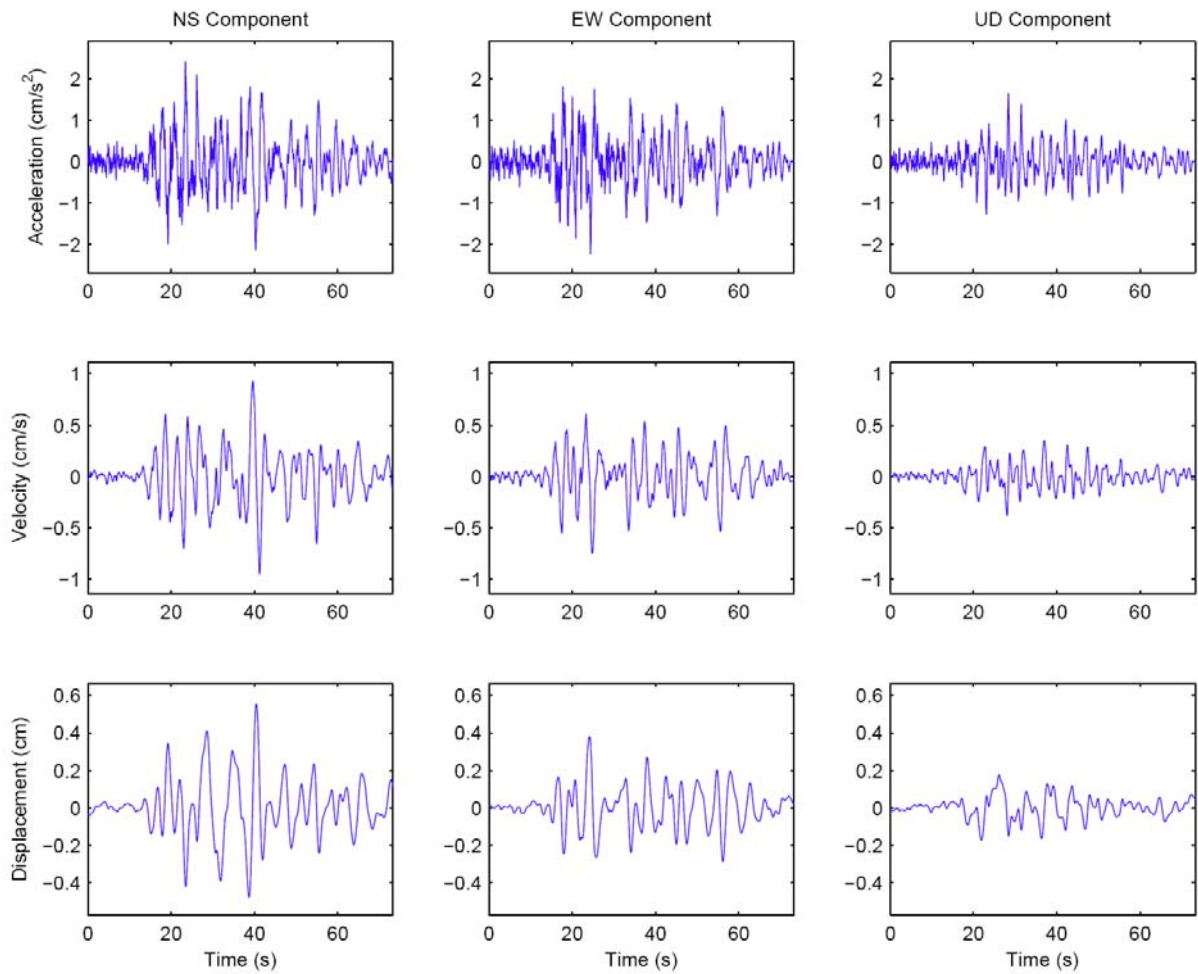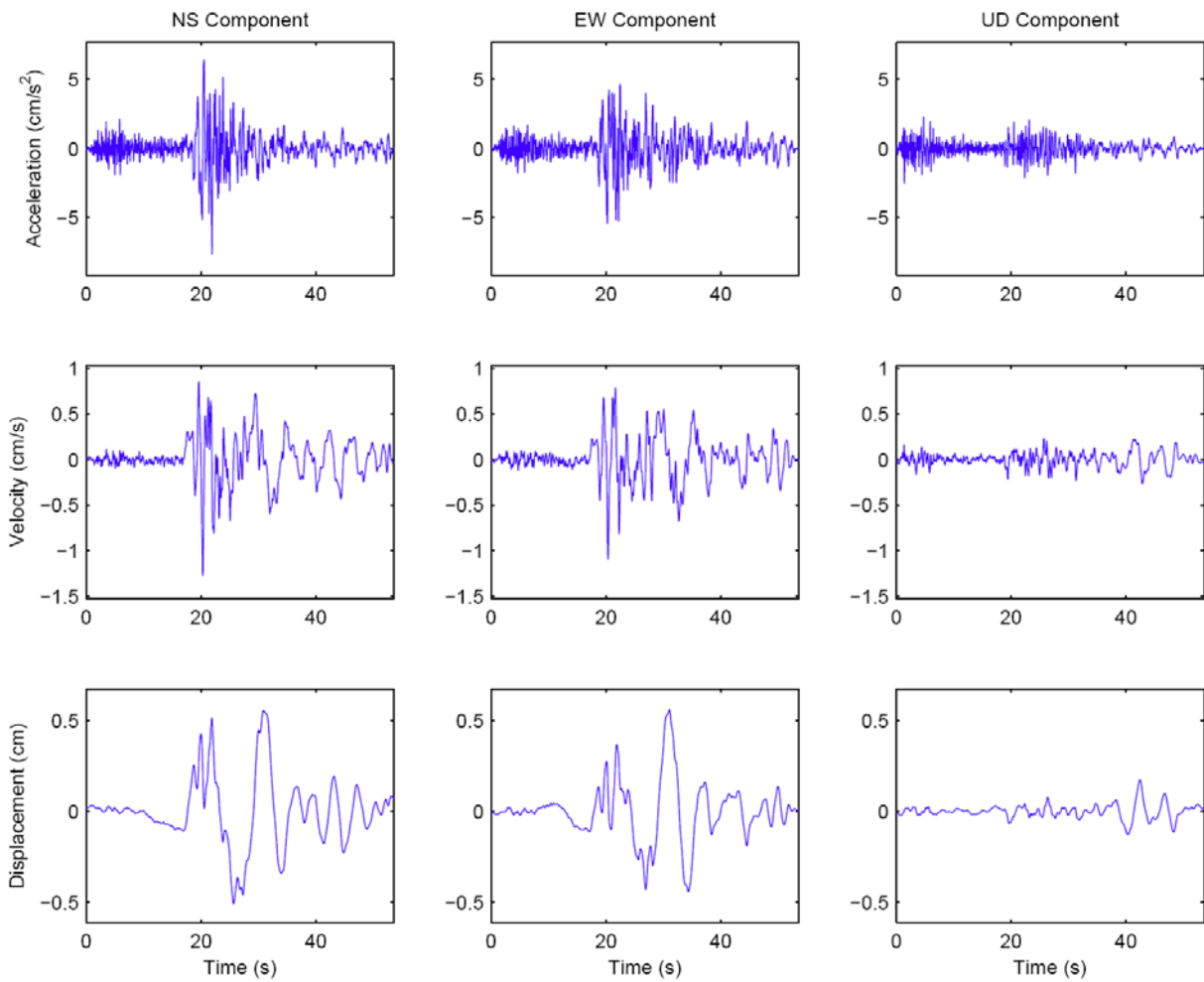
Figure 6. Acceleration (top row), velocity (middle row) and displacement (bottom row) time series of the processed ground motions recorded at Adıyaman-Merkez (Record Name: 20100308023229_0201, Station Code: 0201). The waveforms are band-pass filtered by acausal 4-pole/4-pole Butterworth filter. Zero pads due to acausal filter transients are not shown for illustrative purposes.
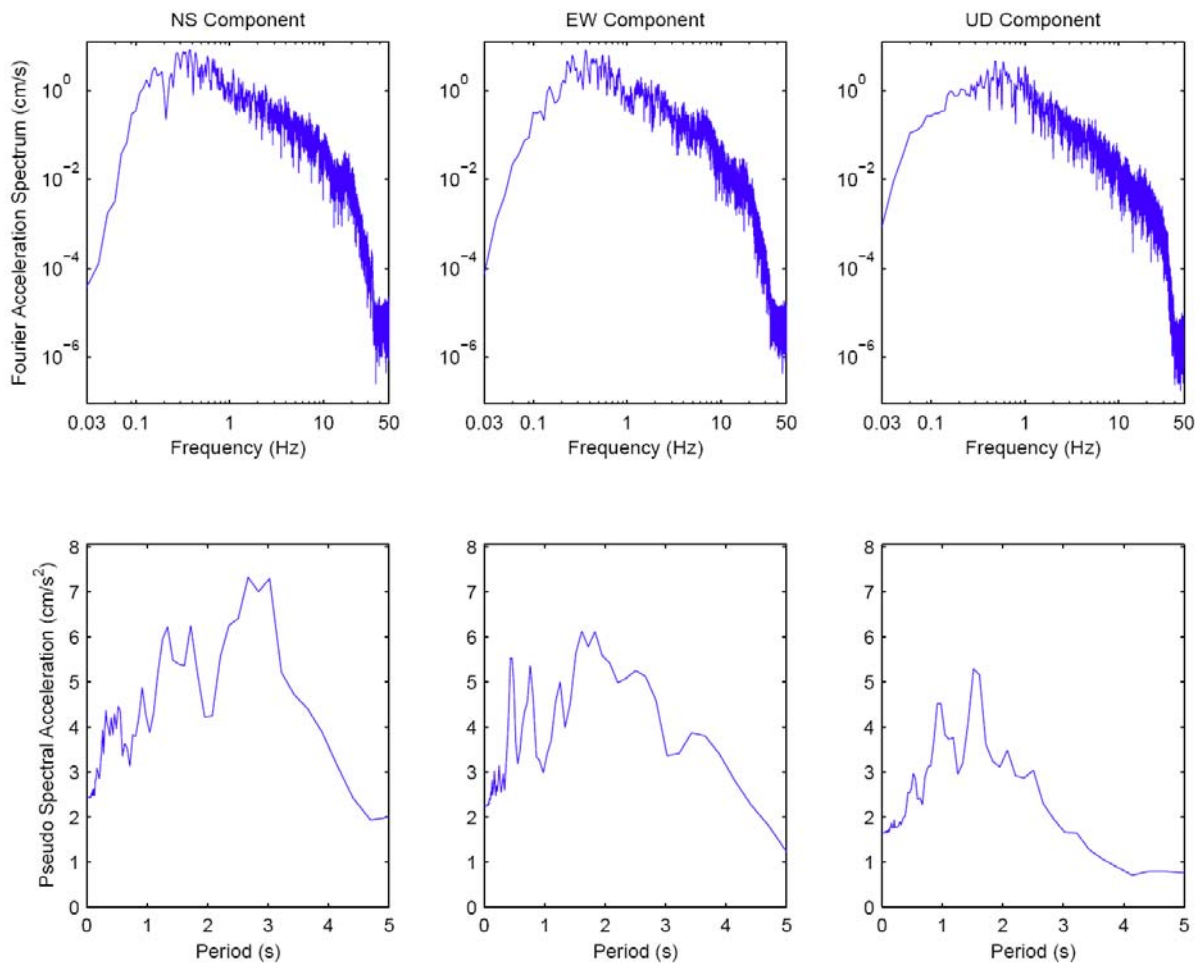
Figure 7. Fourier acceleration spectra (top row) and 5-percent damped pseudo-spectral accelerations (bottom row) of the processed ground motions recorded at Adıyaman-Merkez (Record Name: 20100308023229_0201, Station Code: 0201).

Figure 8. Acceleration (top row), velocity (middle row) and displacement (bottom row) time series of the processed ground motions recorded at Bingöl-Merkez (Record Name: 20100308023229_1201, Station Code: 1201). The waveforms are band-pass filtered by acausal 4-pole/4-pole Butterworth filter. Zero pads due to acausal filter transients are not shown for illustrative purposes.
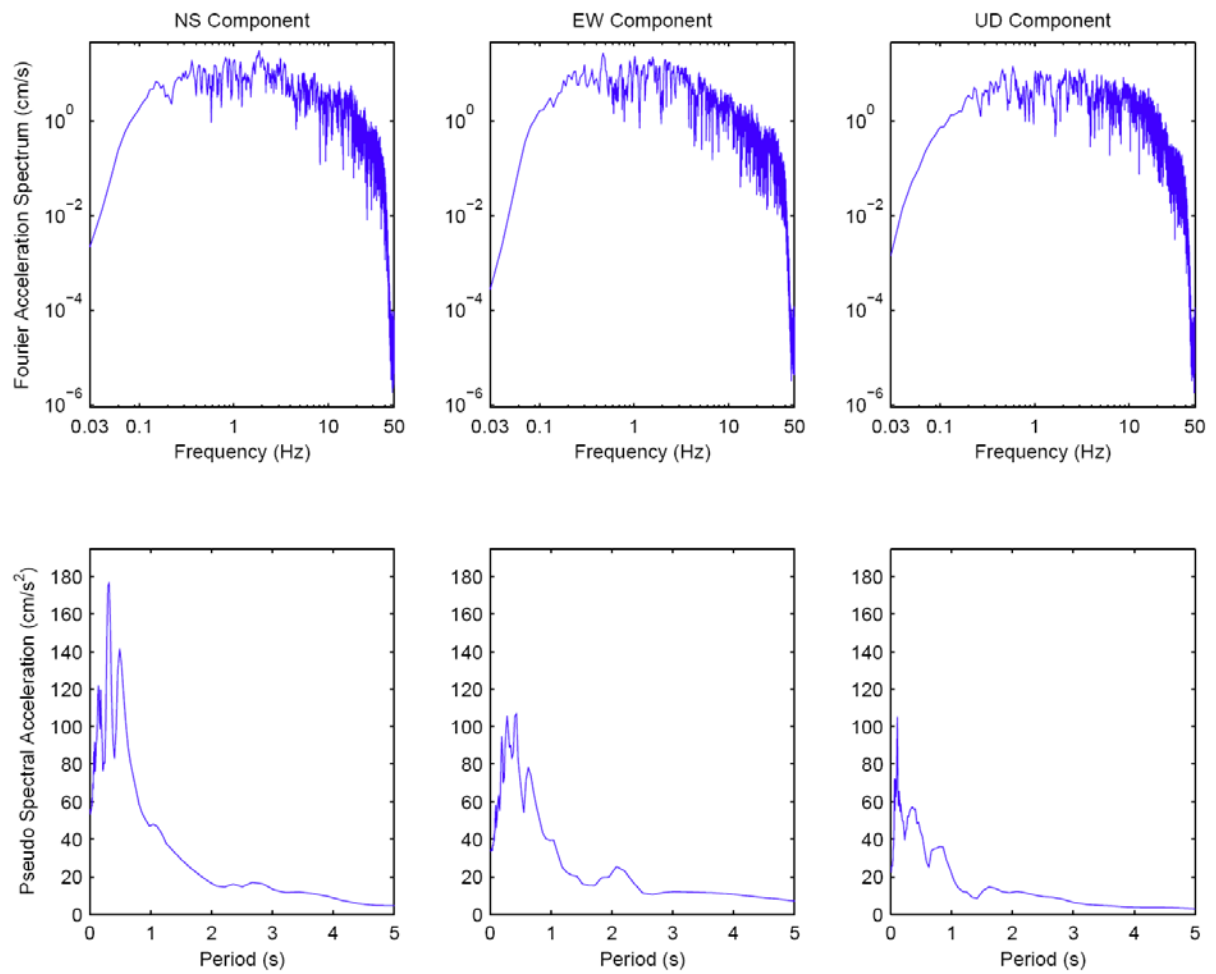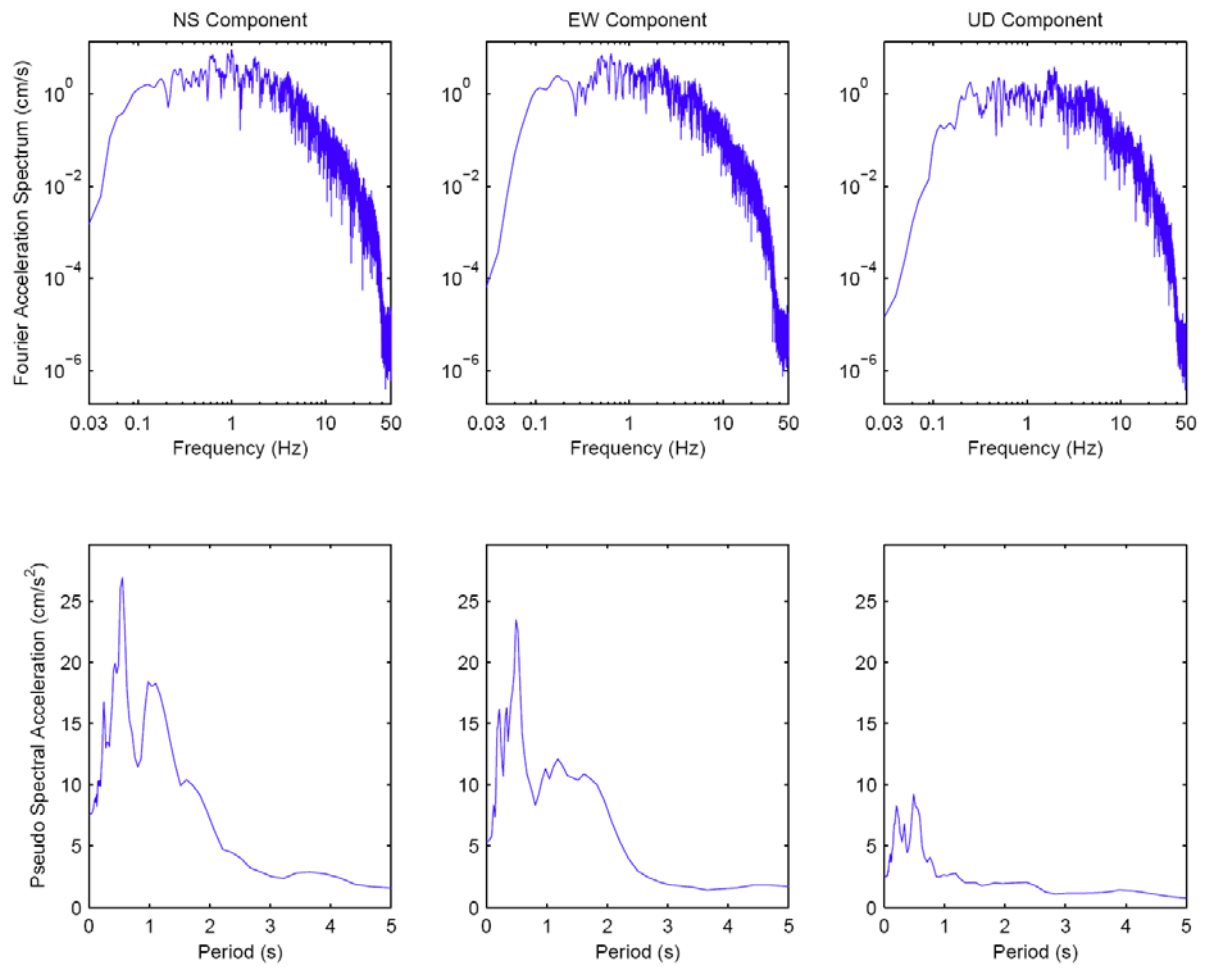
Figure 9. Fourier acceleration spectra (top row) and 5-percent damped pseudo-spectral accelerations (bottom row) of the processed ground motions recorded at Bingöl-Merkez (Record Name: 20100308023229_1201, Station Code: 1201).
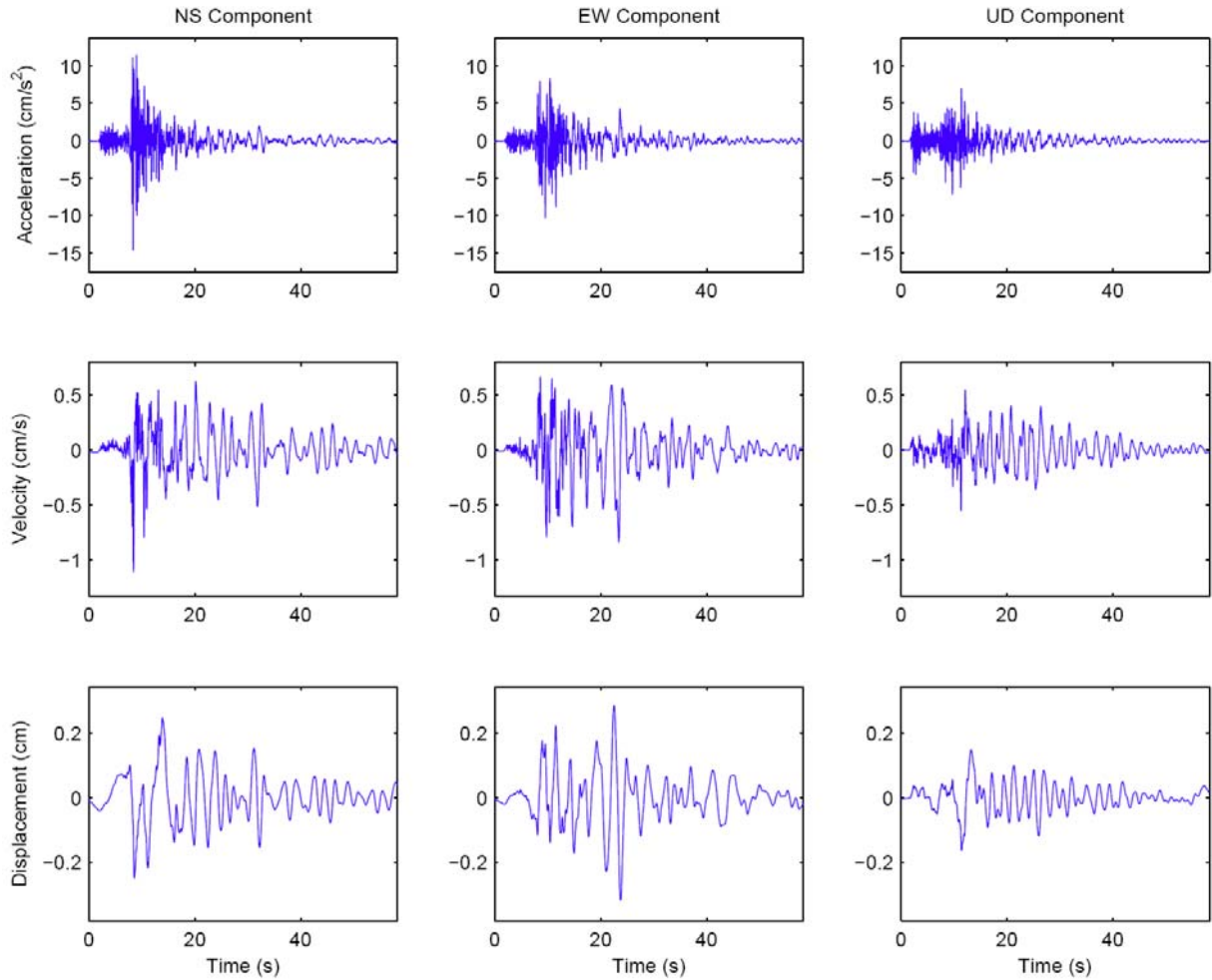
Figure 10. Acceleration (top row), velocity (middle row) and displacement (bottom row) time series of the processed ground motions recorded at Bingöl-Karlıova (Record Name: 20100308023229_1206, Station Code: 1206). The waveforms are band-pass filtered by acausal 4-pole/4-pole Butterworth filter. Zero pads due to acausal filter transients are not shown for illustrative purposes.
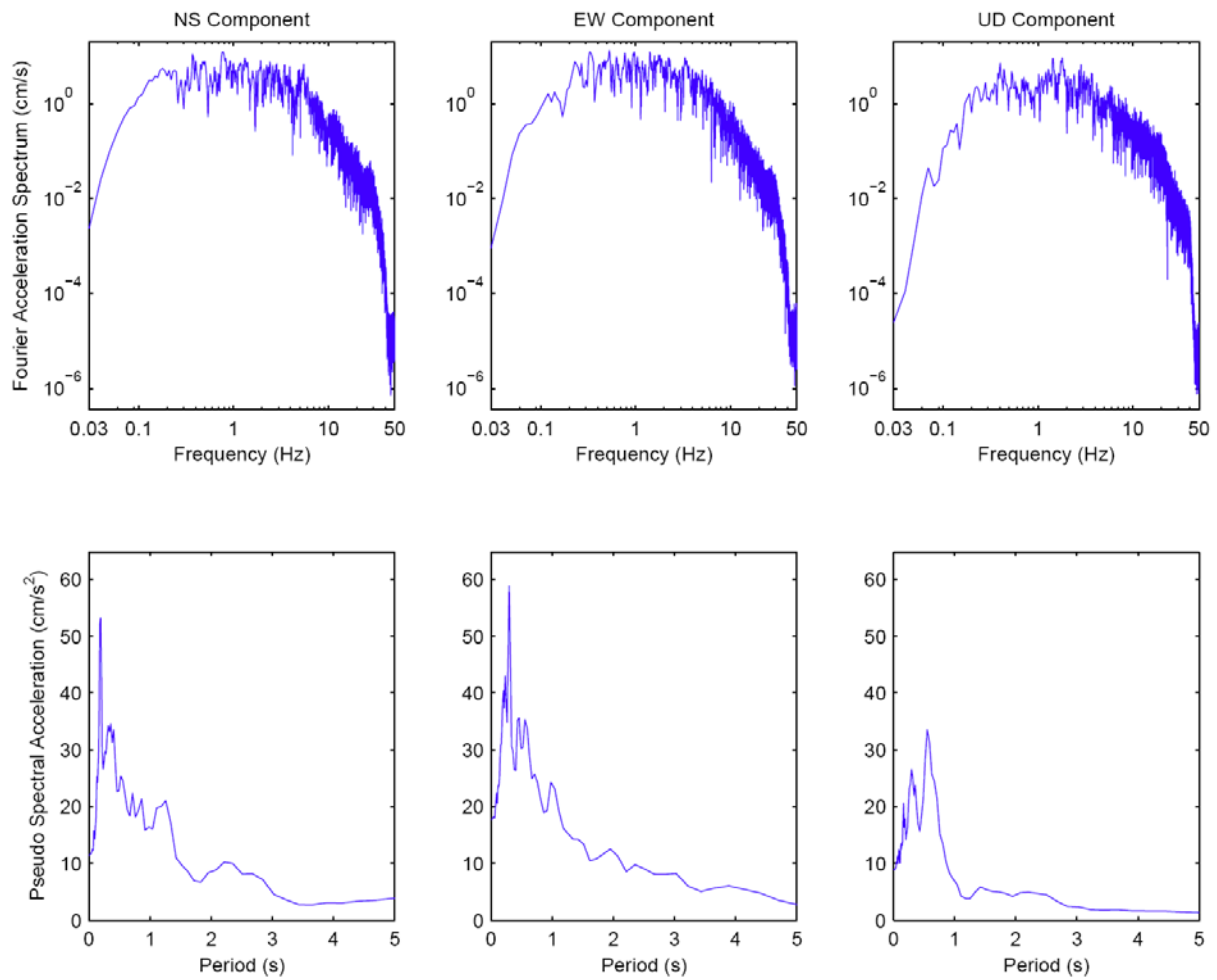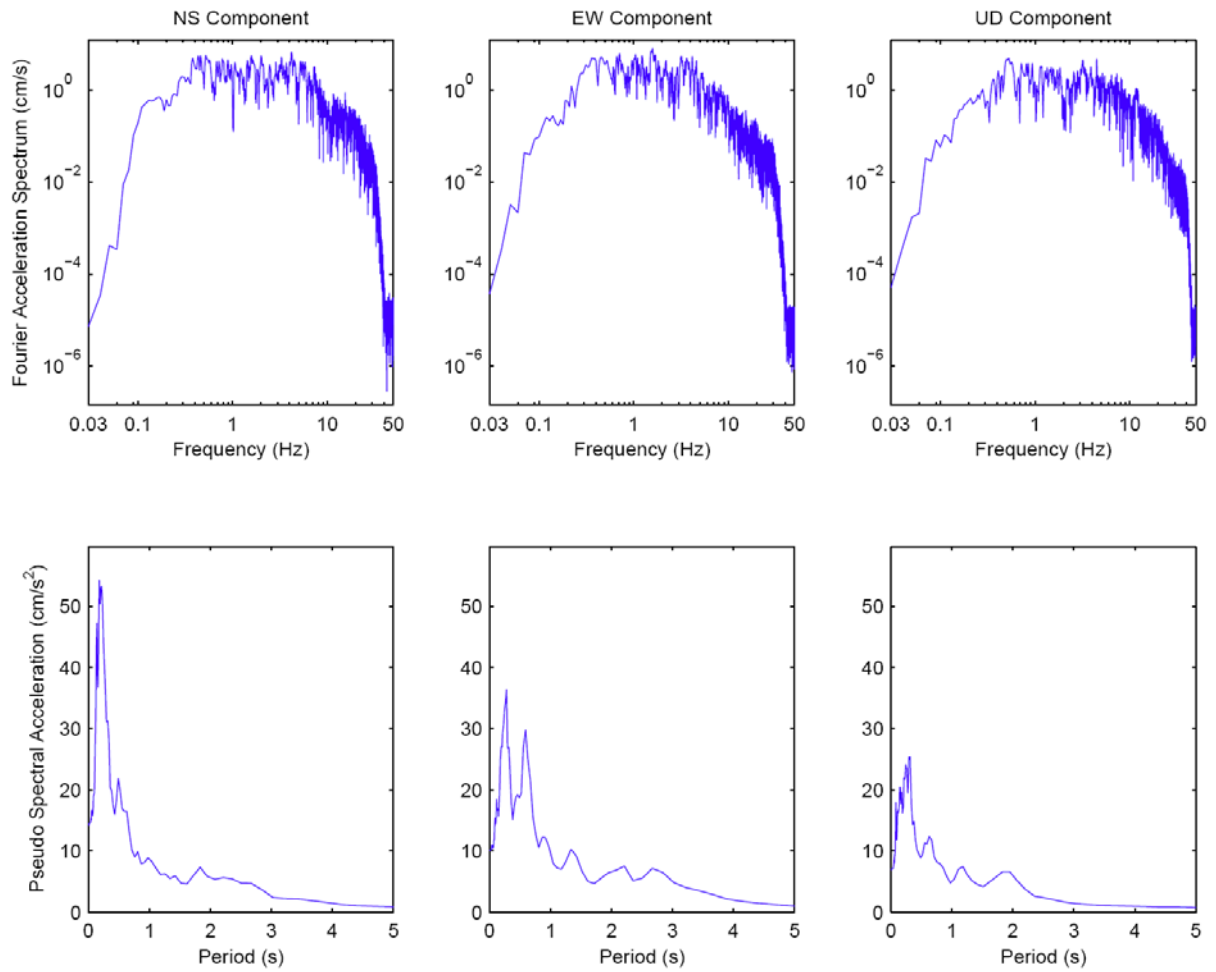
Figure 11. Fourier acceleration spectra (top row) and 5-percent damped pseudo-spectral accelerations (bottom row) of the processed ground motions recorded at Bingöl-Karlıova (Record Name: 20100308023229_1206, Station Code: 1206).
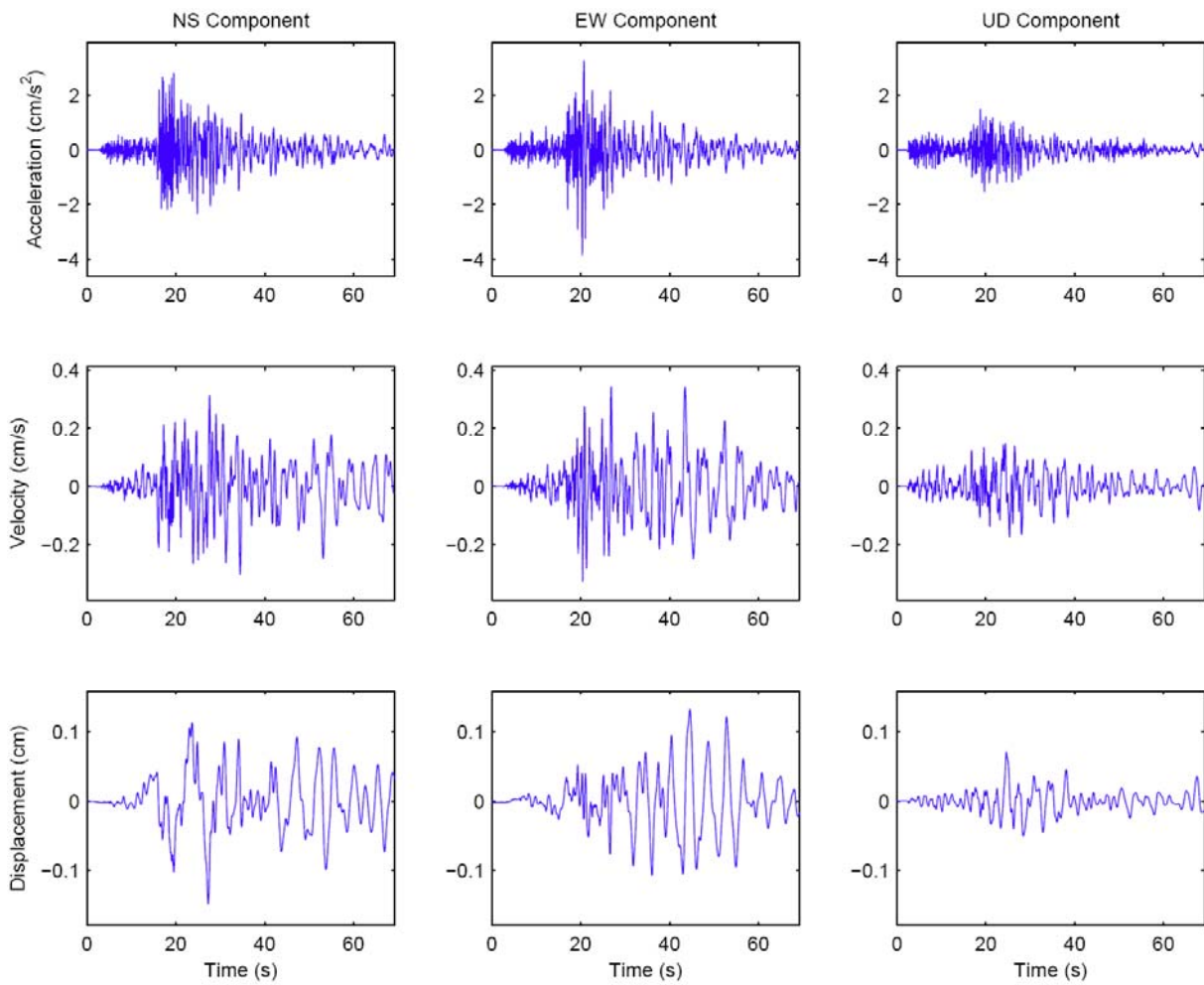
Figure 12. Acceleration (top row), velocity (middle row) and displacement (bottom row) time series of the processed ground motions recorded at Diyarbakır-Merkez (Record Name: 20100308023229_2101, Station Code: 2101). The waveforms are band-pass filtered by acausal 4-pole/4-pole Butterworth filter. Zero pads due to acausal filter transients are not shown for illustrative purposes.

Figure 13. Fourier acceleration spectra (top row) and 5-percent damped pseudo-spectral accelerations (bottom row) of the processed ground motions recorded at Diyarbakır-Merkez (Record Name: 20100308023229_2101, Station Code: 2101).

Figure 14. Acceleration (top row), velocity (middle row) and displacement (bottom row) time series of the processed ground motions recorded at Mardin-Merkez (Record Name: 20100308023229_4701, Station Code: 4701). The waveforms are band-pass filtered by acausal 4-pole/4-pole Butterworth filter. Zero pads due to acausal filter transients are not shown for illustrative purposes.
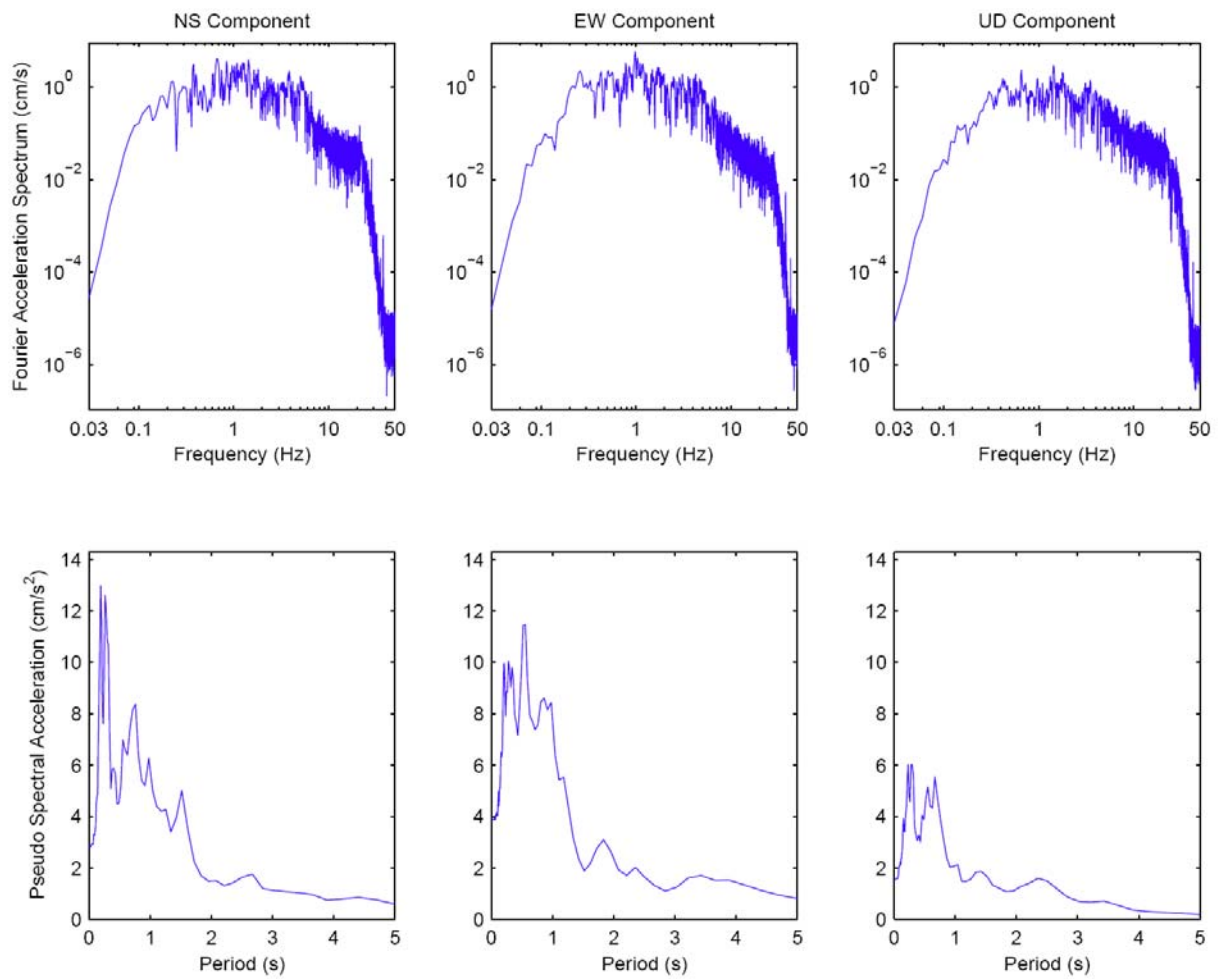
Figure 15. Fourier acceleration spectra (top row) and 5-percent damped pseudo-spectral accelerations (bottom row) of the processed ground motions recorded at Mardin-Merkez (Record Name: 20100308023229_4701, Station Code: 4701).
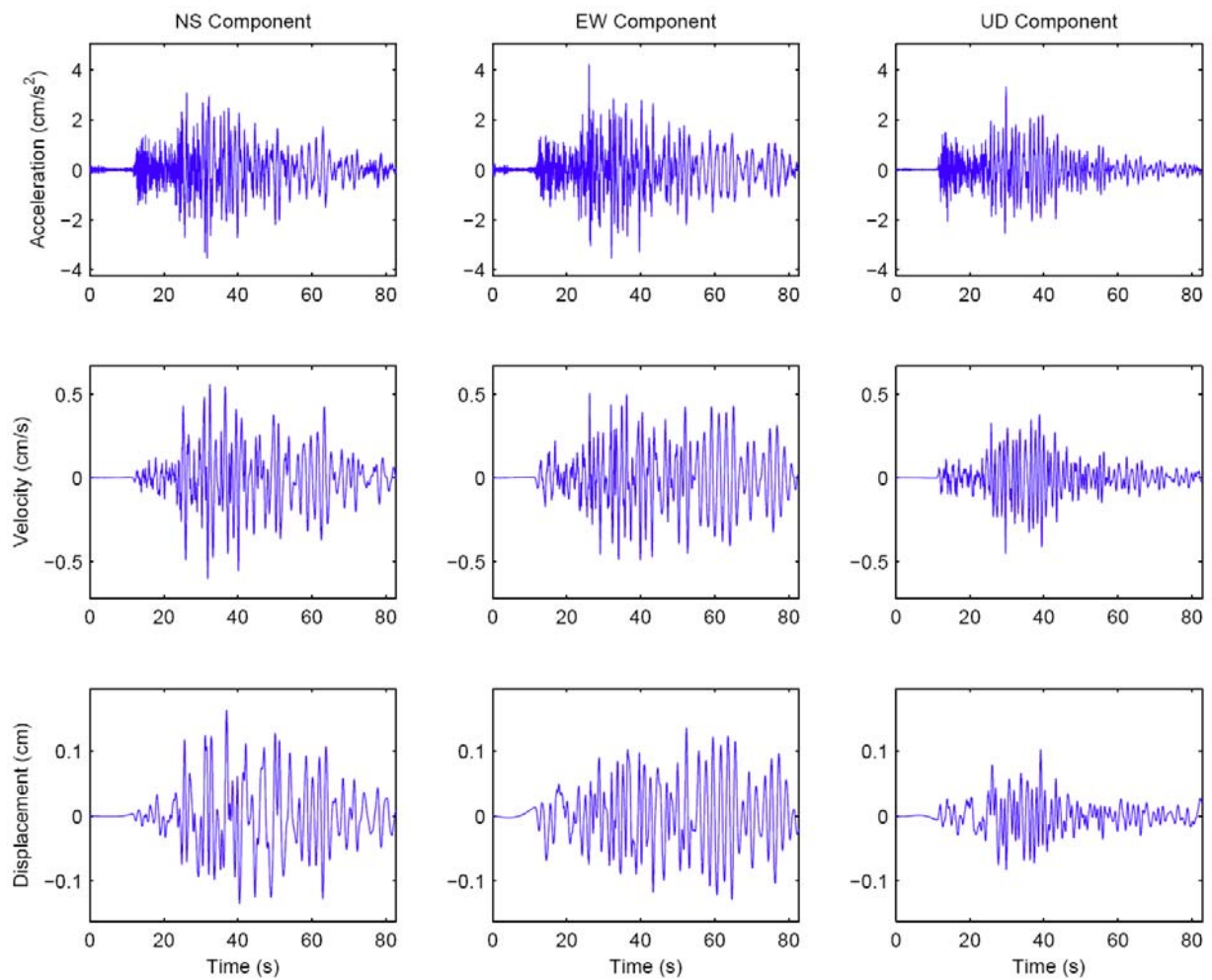
Figure 16. Acceleration (top row), velocity (middle row) and displacement (bottom row) time series of the processed ground motions recorded at Batman-Merkez (Record Name: 20100308023229_7201, Station Code: 7201). The waveforms are band-pass filtered by acausal 4-pole/4-pole Butterworth filter. Zero pads due to acausal filter transients are not shown for illustrative purposes.
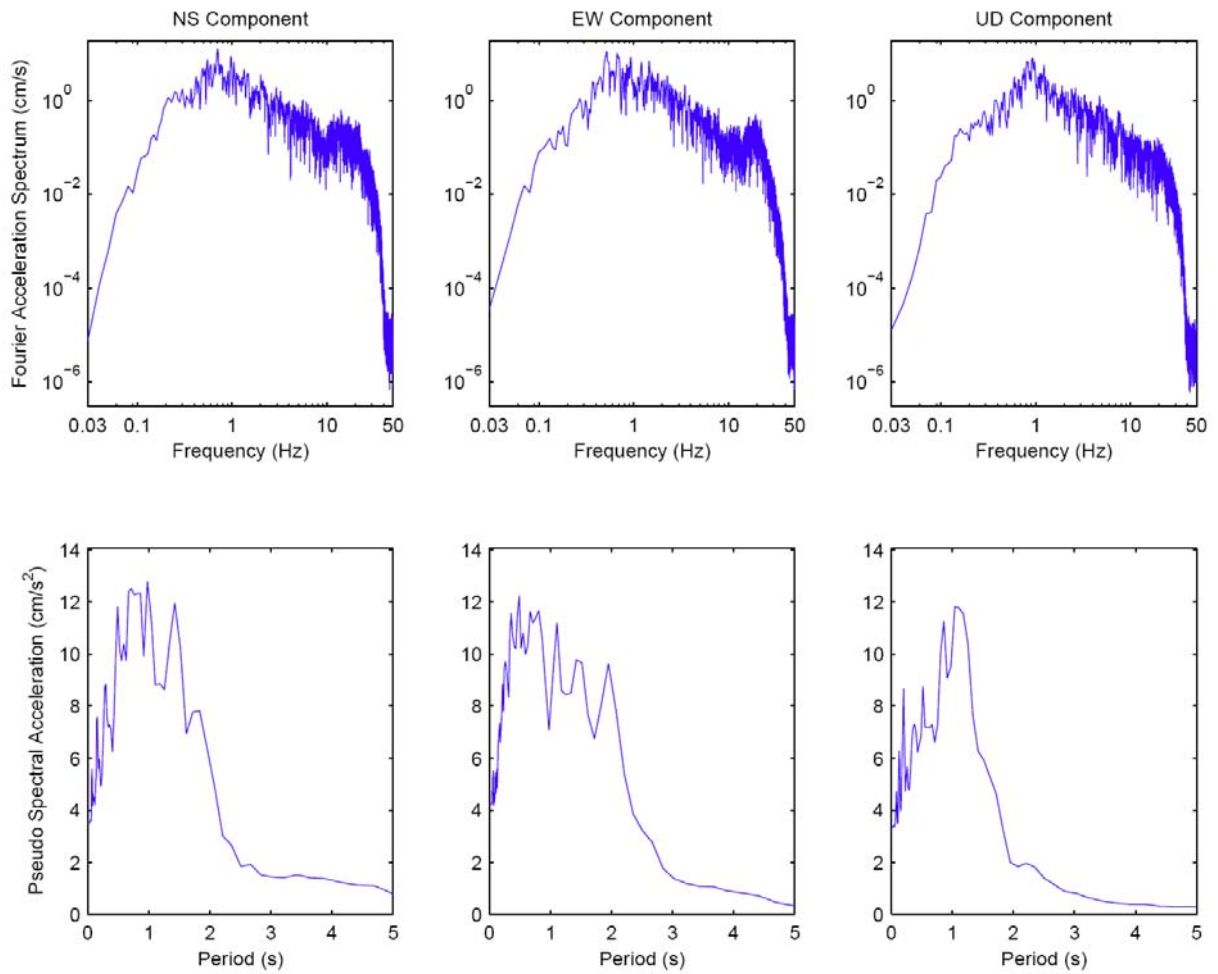
Figure 17. Fourier acceleration spectra (top row) and 5-percent damped pseudo-spectral accelerations (bottom row) of the processed ground motions recorded at Batman-Merkez (Record Name: 20100308023229_7201, Station Code: 7201).

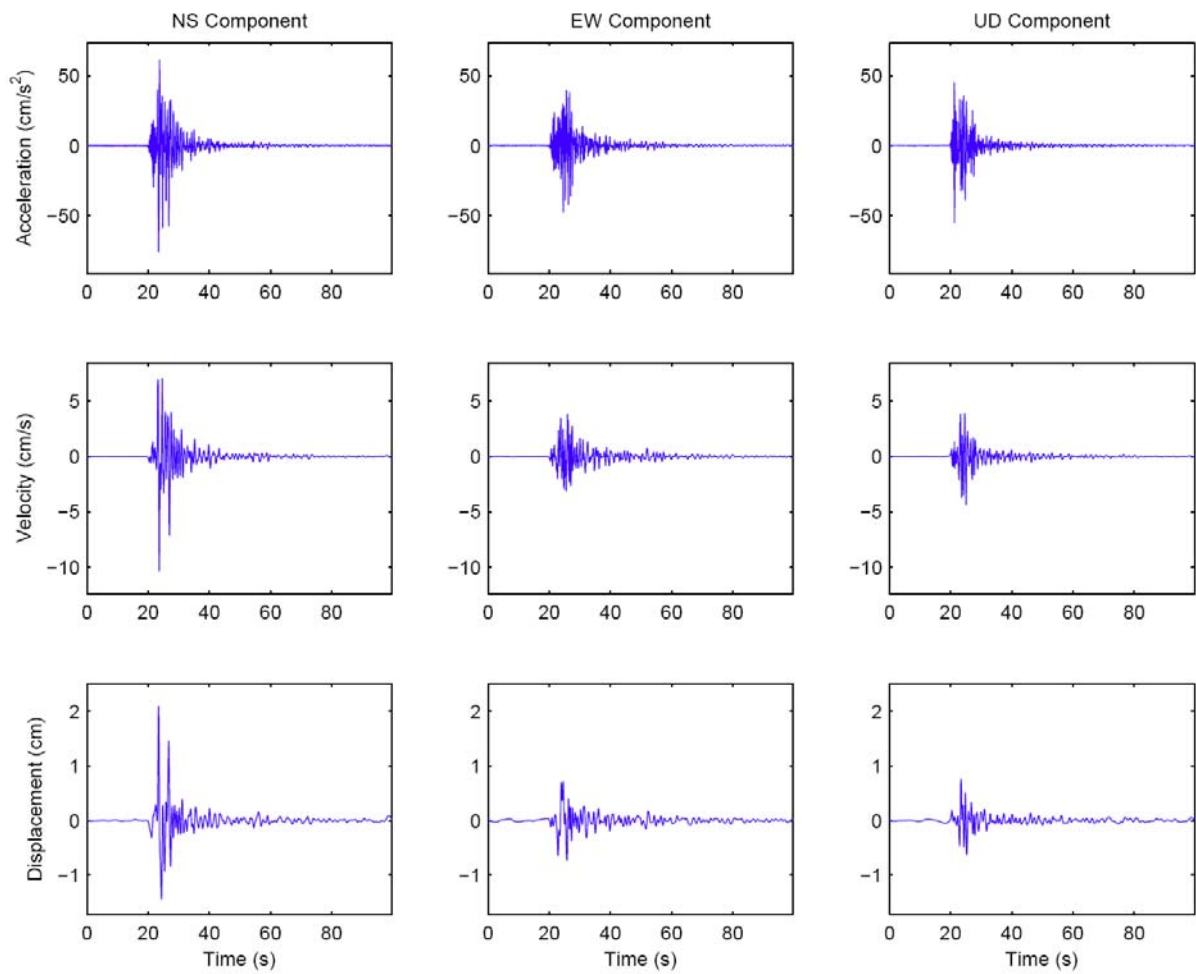**Ground Motions of the 08/03/2010 07:47:37 Elazığ-Palu, Earthquake**



Figure 18. Acceleration (top row), velocity (middle row) and displacement (bottom row) time series of the processed ground motions recorded at Bingöl-Merkez (Record Name: 20100308074737_1201, Station Code: 1201). The waveforms are band-pass filtered by acausal 4-pole/4-pole Butterworth filter. Zero pads due to acausal filter transients are not shown for illustrative purposes.
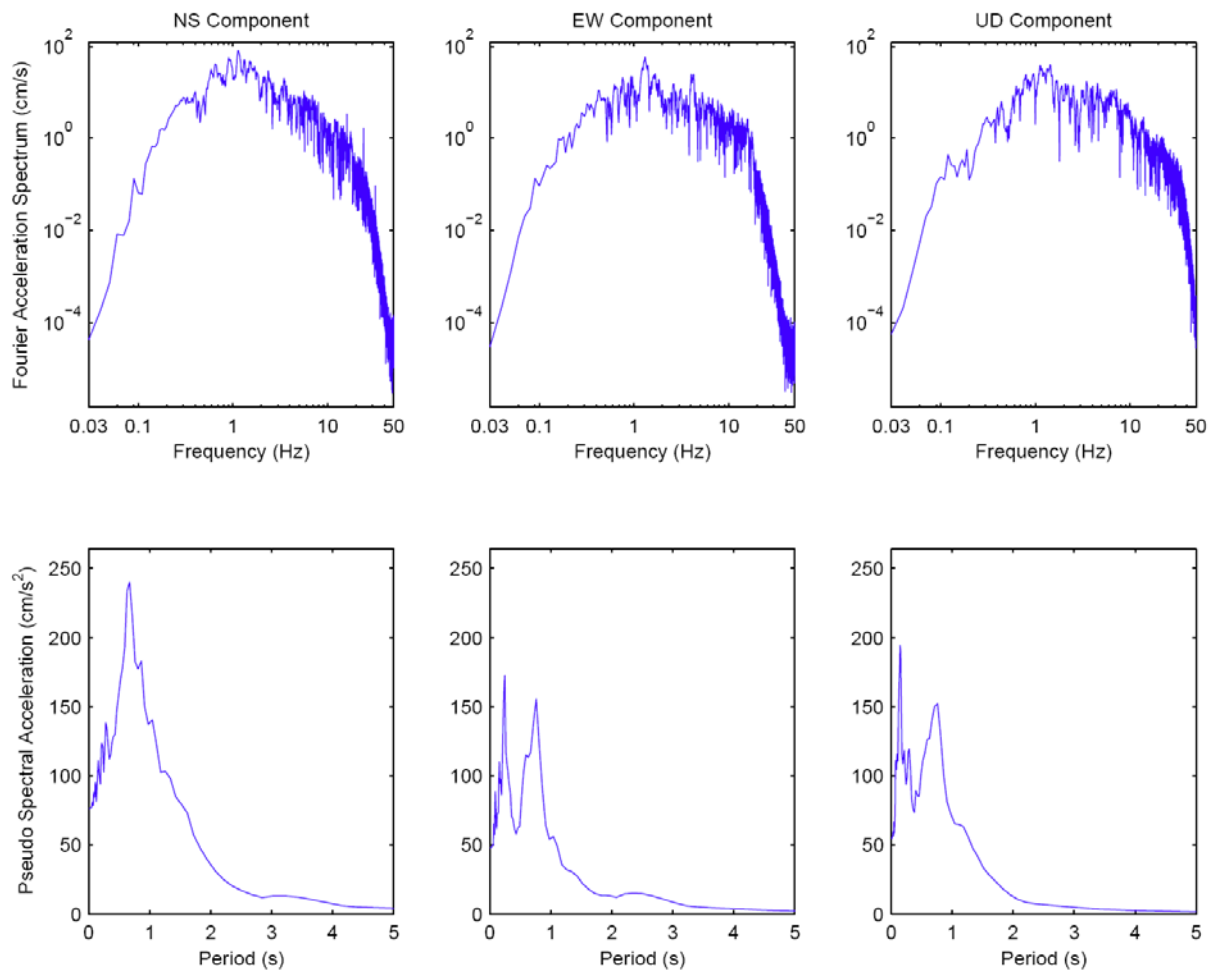
Figure 19. Fourier acceleration spectra (top row) and 5-percent damped pseudo-spectral accelerations (bottom row) of the processed ground motions recorded at Bingöl-Merkez (Record Name: 20100308074737_1201, Station Code: 1201).
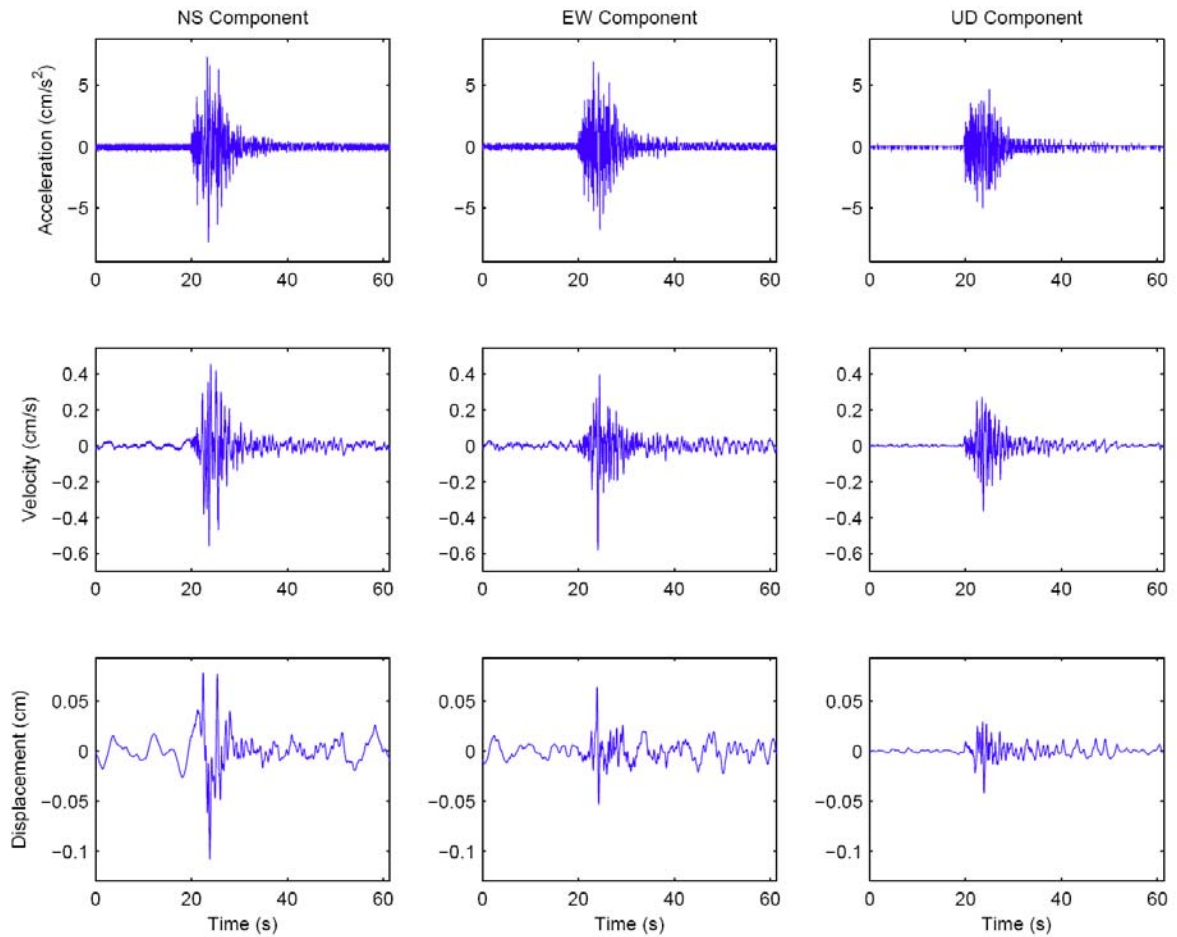
Figure 20. Acceleration (top row), velocity (middle row) and displacement (bottom row) time series of the processed ground motions recorded at Bingöl-Karlıova (Record Name: 20100308074737_1206, Station Code: 1206). The waveforms are band-pass filtered by acausal 4-pole/4-pole Butterworth filter. Zero pads due to acausal filter transients are not shown for illustrative purposes.

Figure 21. Fourier acceleration spectra (top row) and 5-percent damped pseudo-spectral accelerations (bottom row) of the processed ground motions recorded at Bingöl-Karlıova (Record Name: 20100308074737_1206, Station Code: 1206).

Figure 22. Acceleration (top row), velocity (middle row) and displacement (bottom row) time series of the processed ground motions recorded at Elazığ-Merkez (Record Name: 20100308074737_2301, Station Code: 2301). The waveforms are band-pass filtered by acausal 4-pole/4-pole Butterworth filter. Zero pads due to acausal filter transients are not shown for illustrative purposes.
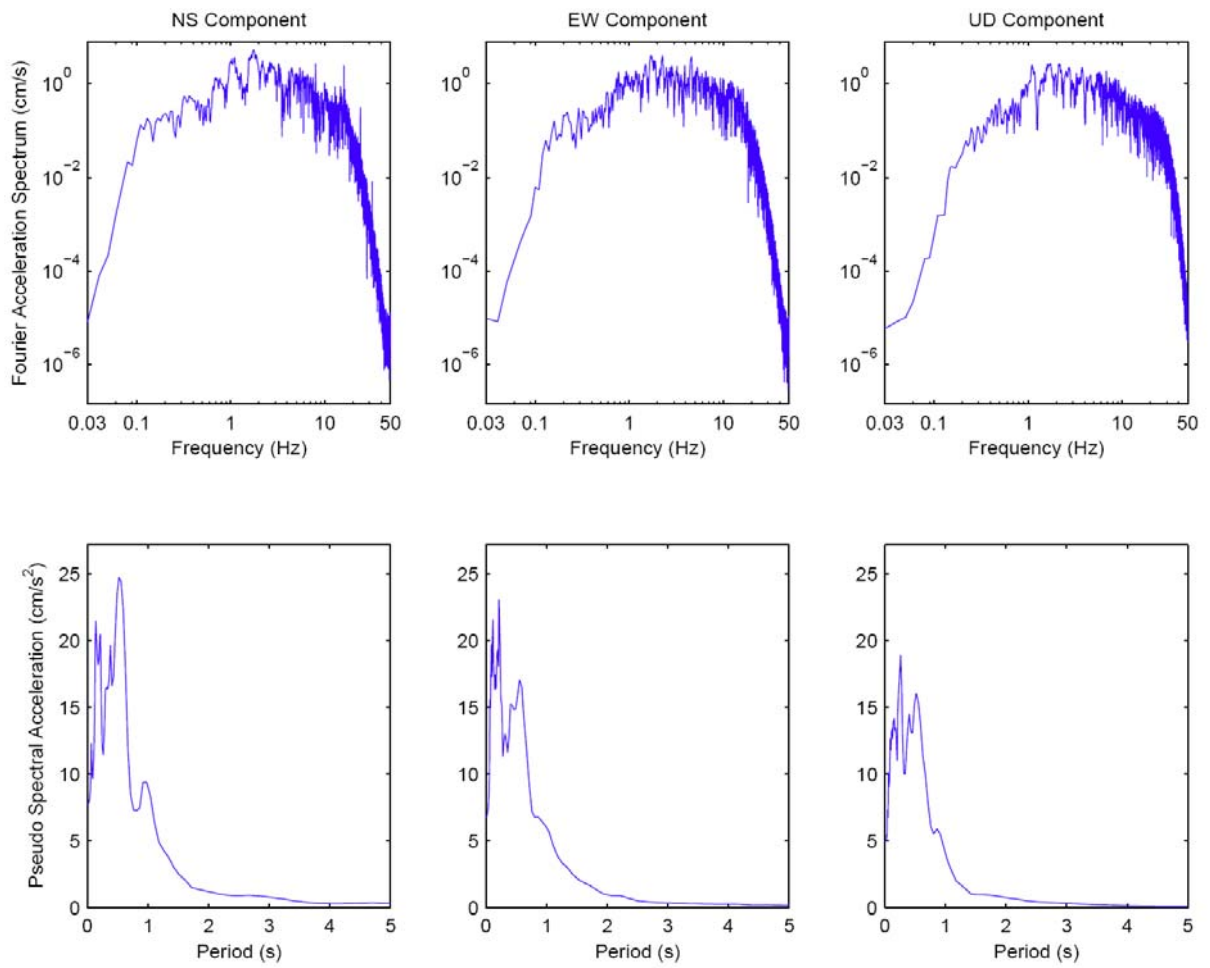
Figure 23. Fourier acceleration spectra (top row) and 5-percent damped pseudo-spectral accelerations (bottom row) of the processed ground motions recorded at Elazığ-Merkez (Record Name: 20100308074737_2301, Station Code: 2301).
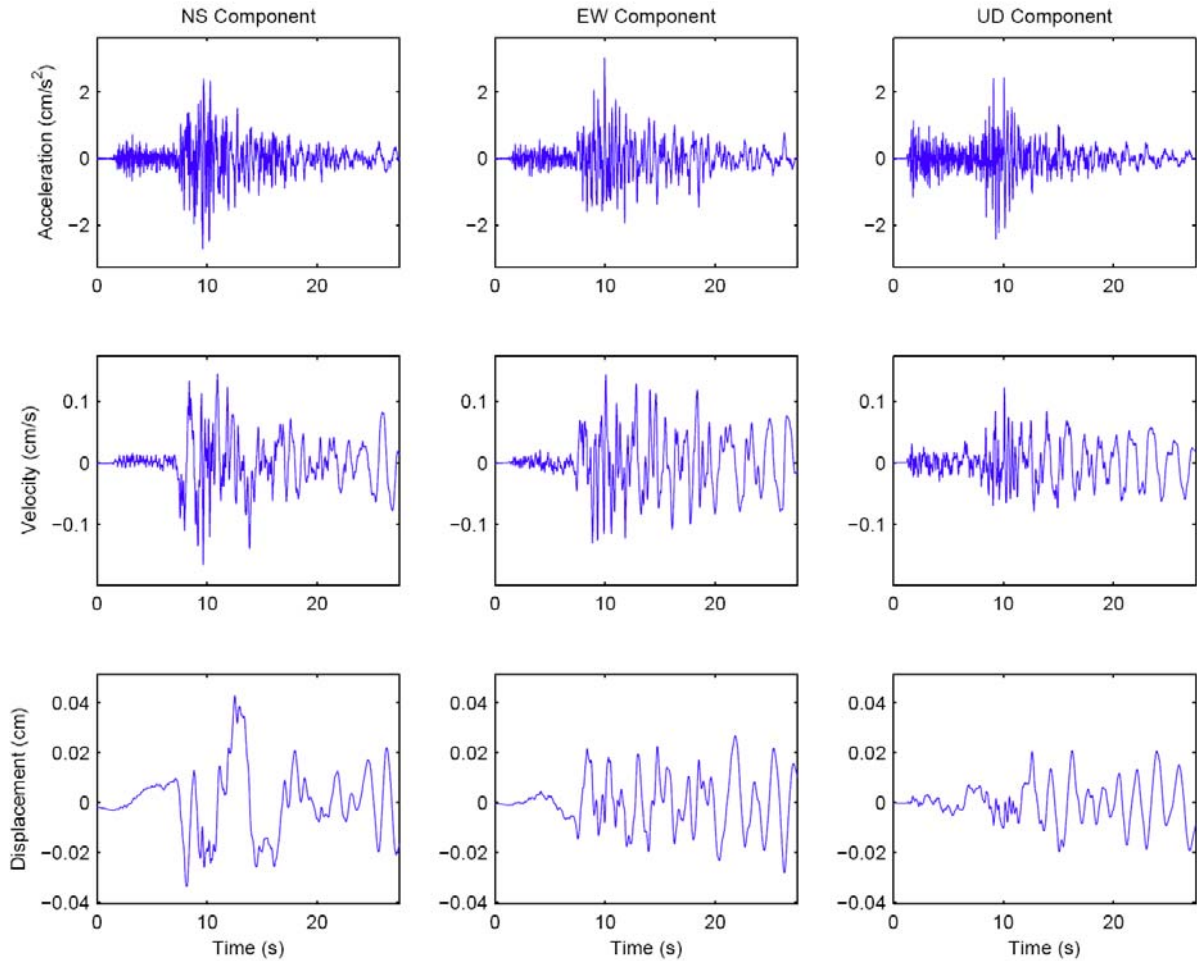
Figure 24. Acceleration (top row), velocity (middle row) and displacement (bottom row) time series of the processed ground motions recorded at Elazığ-Palu (Record Name: 20100308074737_2303, Station Code: 2303). The waveforms are band-pass filtered by acausal 4-pole/4-pole Butterworth filter. Zero pads due to acausal filter transients are not shown for illustrative purposes.
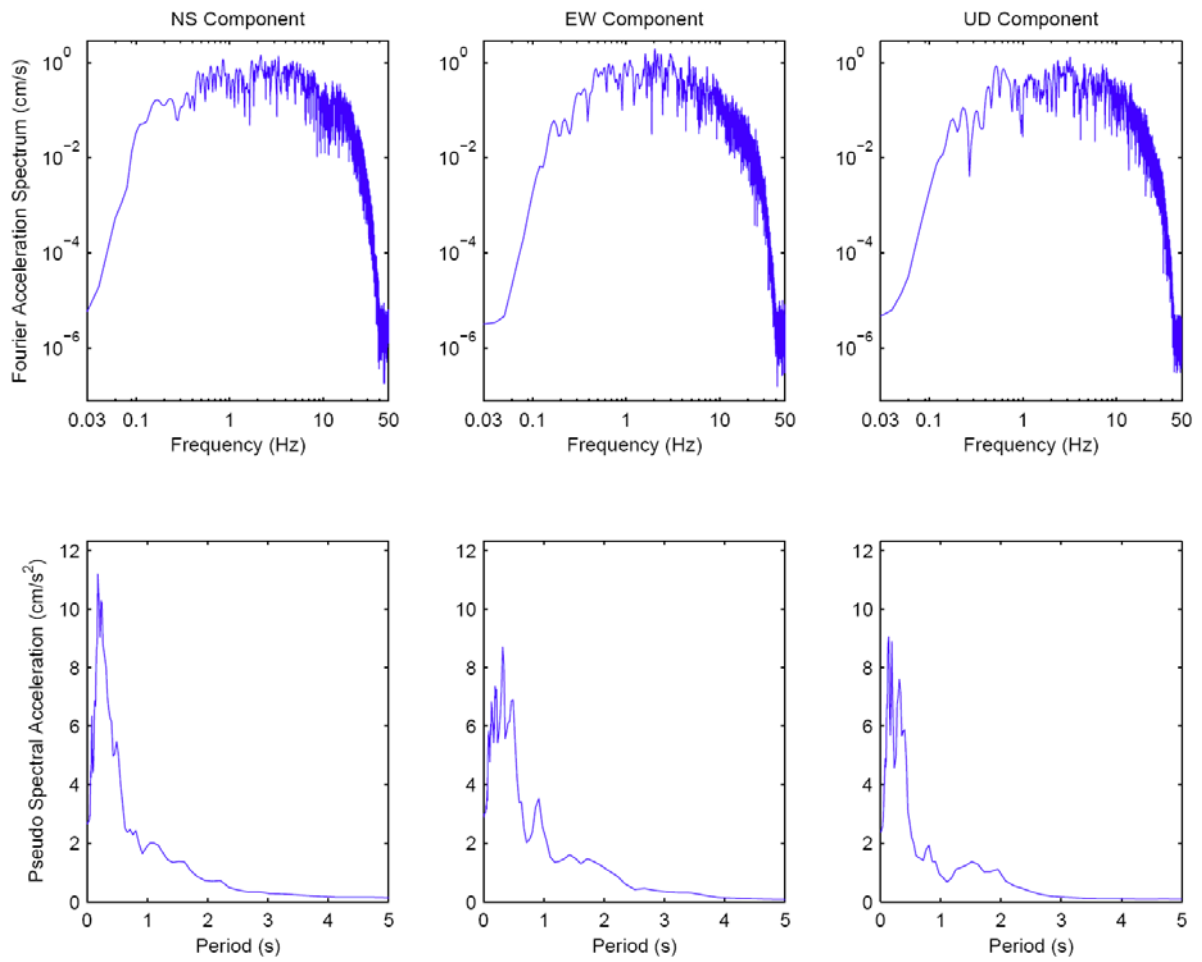
Figure 25. Fourier acceleration spectra (top row) and 5-percent damped pseudo-spectral accelerations (bottom row) of the processed ground motions recorded at Elazığ-Palu (Record Name: 20100308074737_2303, Station Code: 2303).

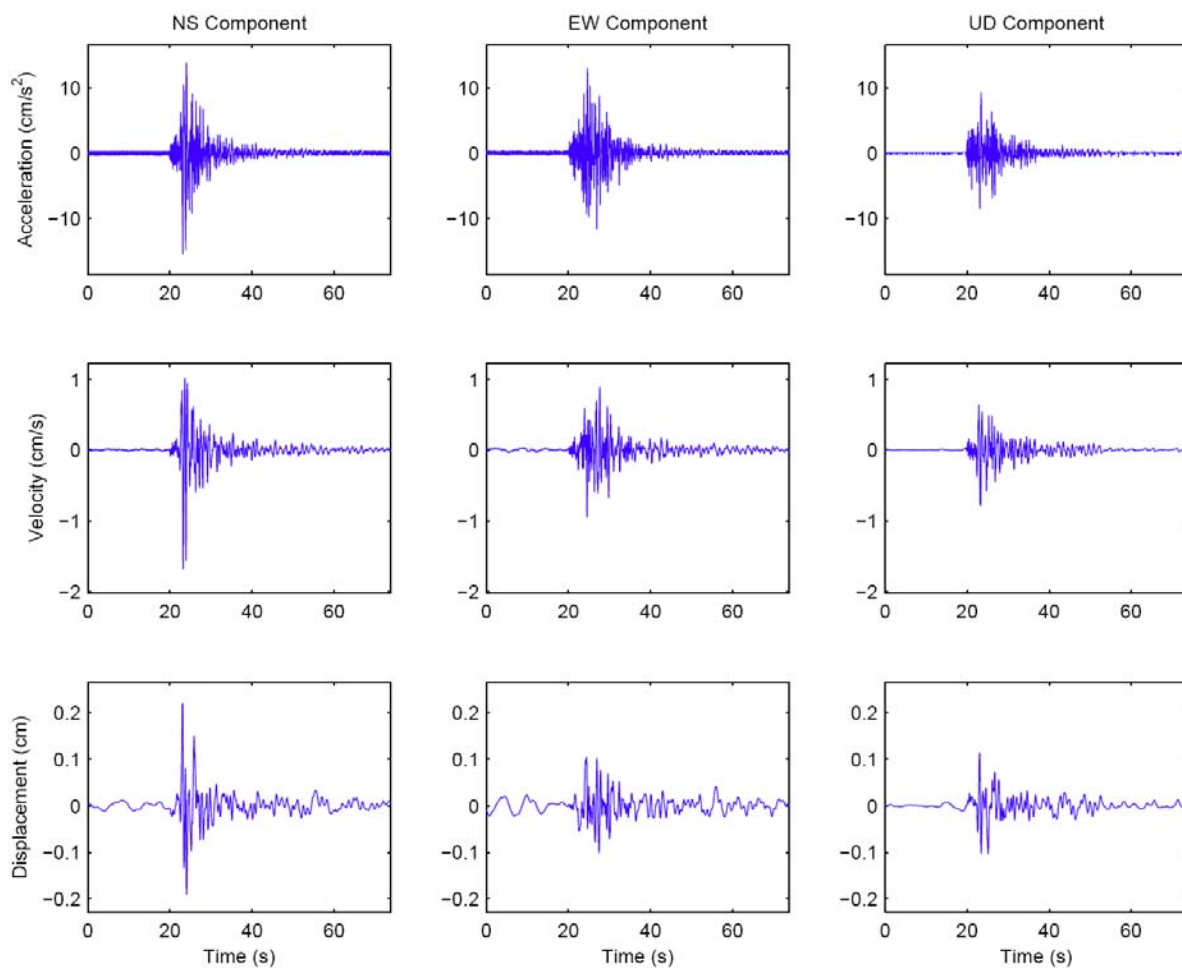**Ground Motions of the 08/03/2010 08:11:20 Elazığ-Palu, Earthquake**



Figure 26. Acceleration (top row), velocity (middle row) and displacement (bottom row) time series of the processed ground motions recorded at Elazığ-Palu (Record Name: 20100308081120_2303, Station Code: 2303). The waveforms are band-pass filtered by acausal 4-pole/4-pole Butterworth filter. Zero pads due to acausal filter transients are not shown for illustrative purposes.

Figure 27. Fourier acceleration spectra (top row) and 5-percent damped pseudo-spectral accelerations (bottom row) of the processed ground motions recorded at Elazığ-Palu (Record Name: 20100308081120_2303, Station Code: 2303).

**Ground Motions of the 08/03/2010 09:00:46 Elazığ-Kovancılar, Earthquake**



Figure 28. Acceleration (top row), velocity (middle row) and displacement (bottom row) time series of the processed ground motions recorded at Bingöl-Merkez (Record Name: 20100308090046_1201, Station Code: 1201). The waveforms are band-pass filtered by acausal 4-pole/4-pole Butterworth filter. Zero pads due to acausal filter transients are not shown for illustrative purposes.
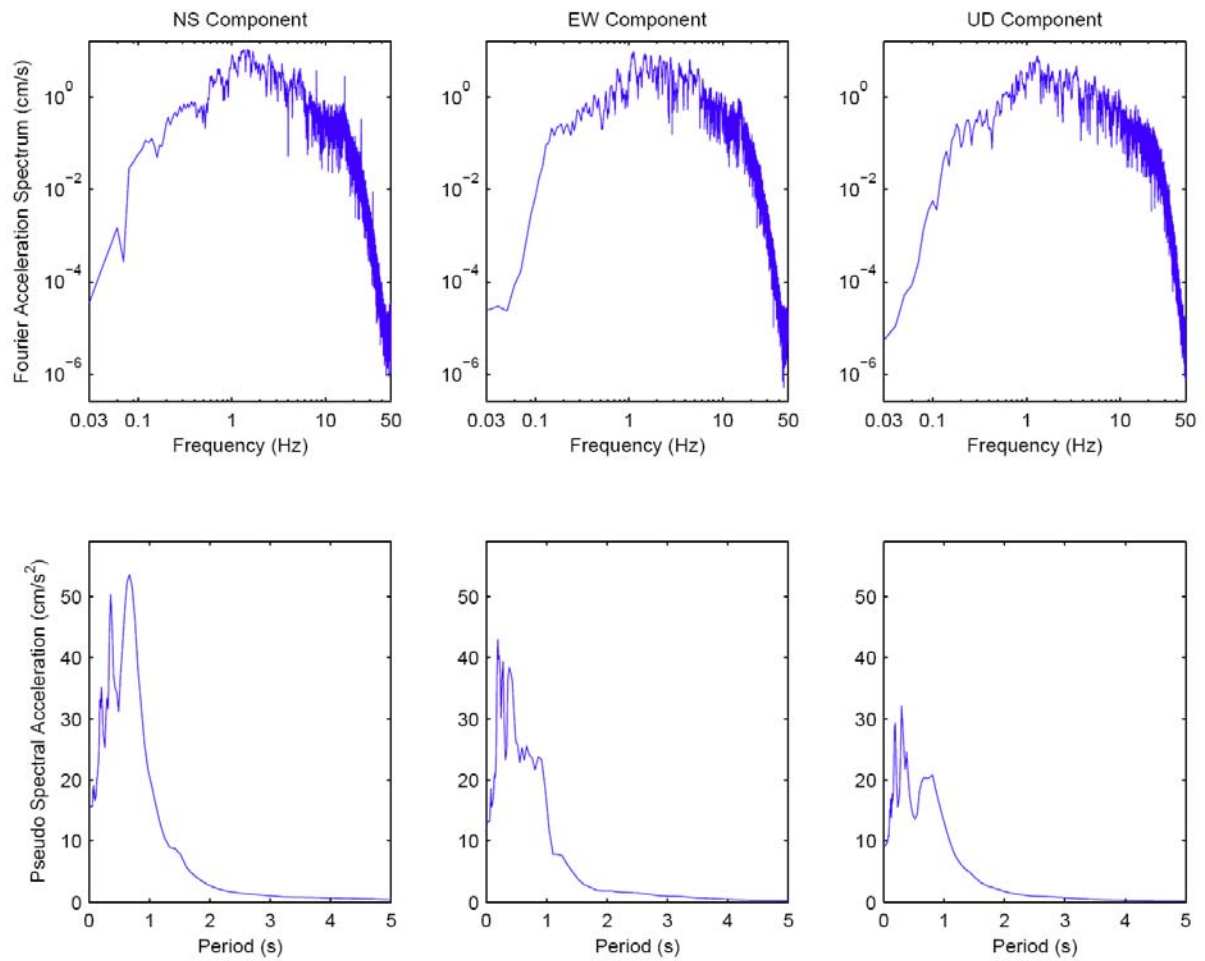
Figure 29. Fourier acceleration spectra (top row) and 5-percent damped pseudo-spectral accelerations (bottom row) of the processed ground motions recorded at Bingöl-Merkez (Record Name: 20100308090046_1201, Station Code: 1201).
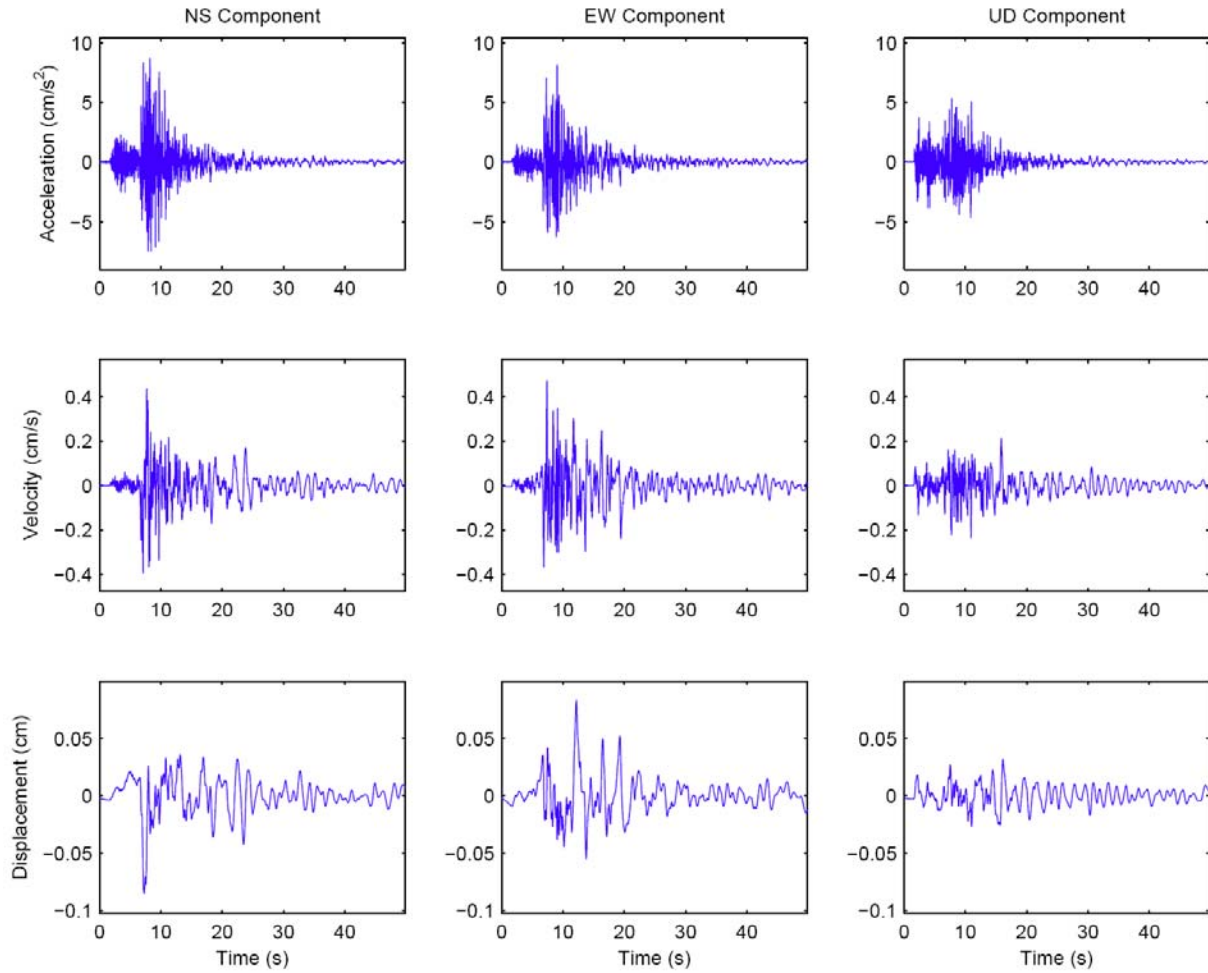
Figure 30. Acceleration (top row), velocity (middle row) and displacement (bottom row) time series of the processed ground motions recorded at Elazığ-Palu (Record Name: 20100308090046_2303, Station Code: 2303). The waveforms are band-pass filtered by acausal 4-pole/4-pole Butterworth filter. Zero pads due to acausal filter transients are not shown for illustrative purposes.
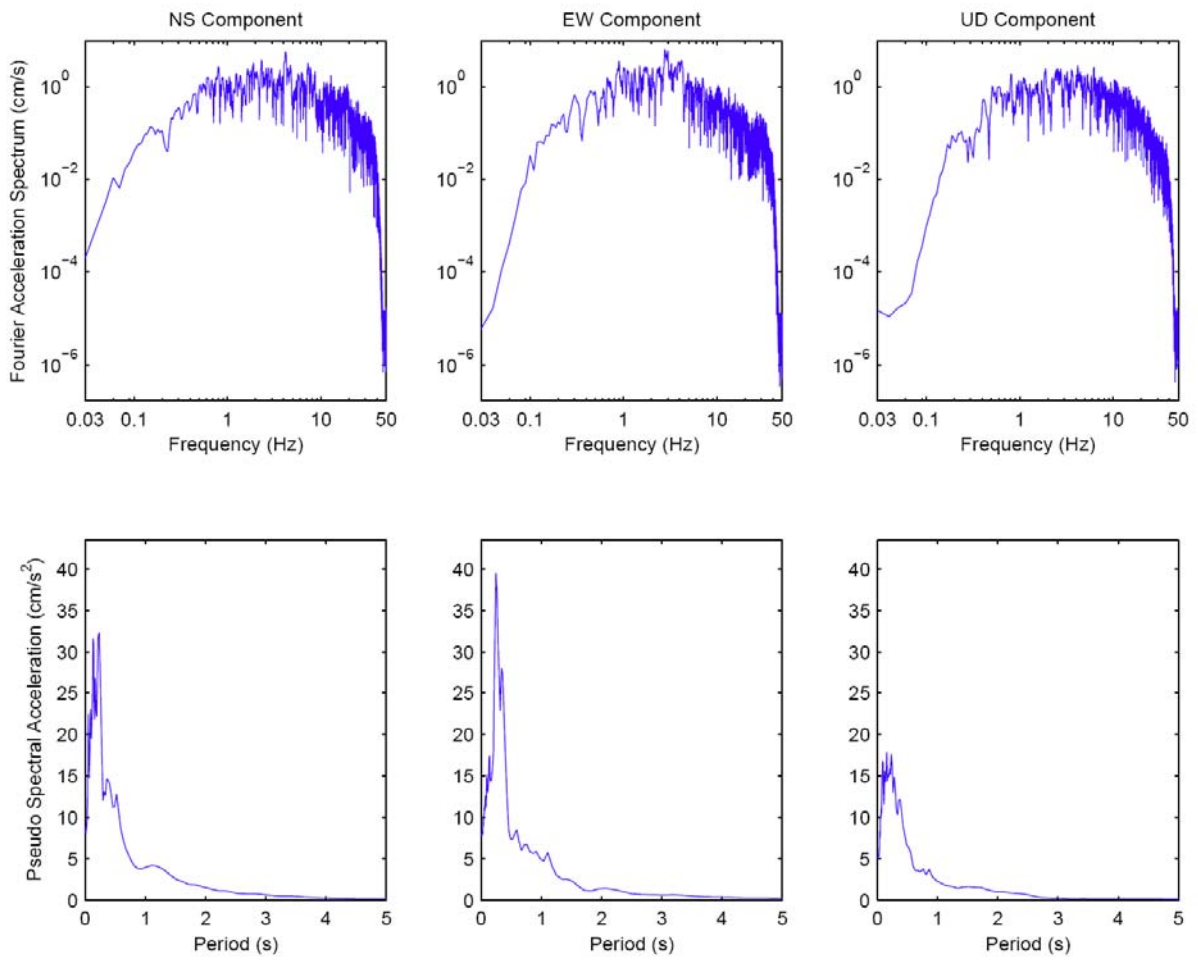
Figure 31. Fourier acceleration spectra (top row) and 5-percent damped pseudo-spectral accelerations (bottom row) of the processed ground motions recorded at Elazığ-Palu (Record Name: 20100308090046_2303, Station Code: 2303).

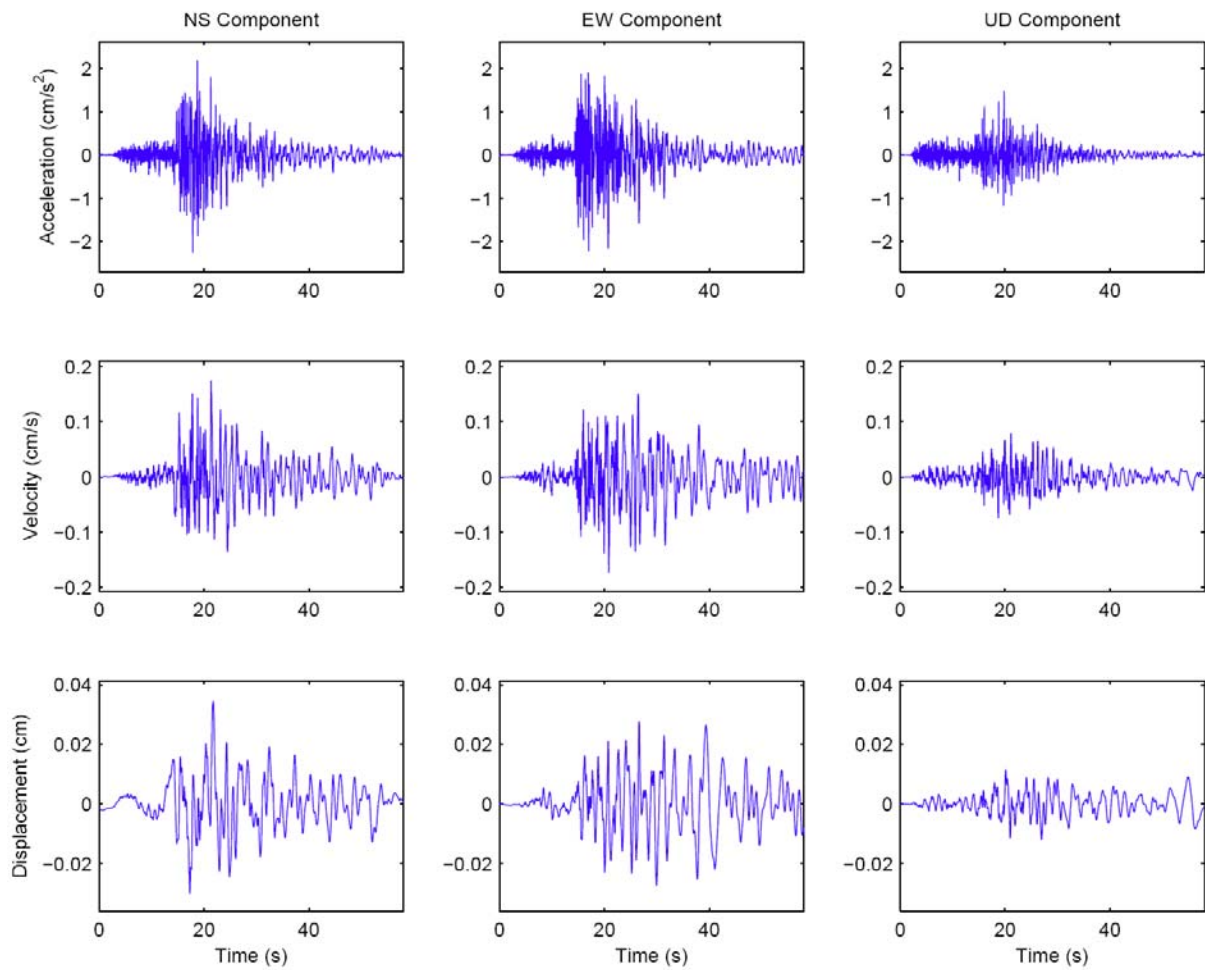**Ground Motions of the 08/03/2010 10:14:23 Elazığ-Kovancılar, Earthquake**



Figure 32. Acceleration (top row), velocity (middle row) and displacement (bottom row) time series of the processed ground motions recorded at Bingöl-Merkez (Record Name: 20100308101423_1201, Station Code: 1201). The waveforms are band-pass filtered by acausal 4-pole/4-pole Butterworth filter. Zero pads due to acausal filter transients are not shown for illustrative purposes.
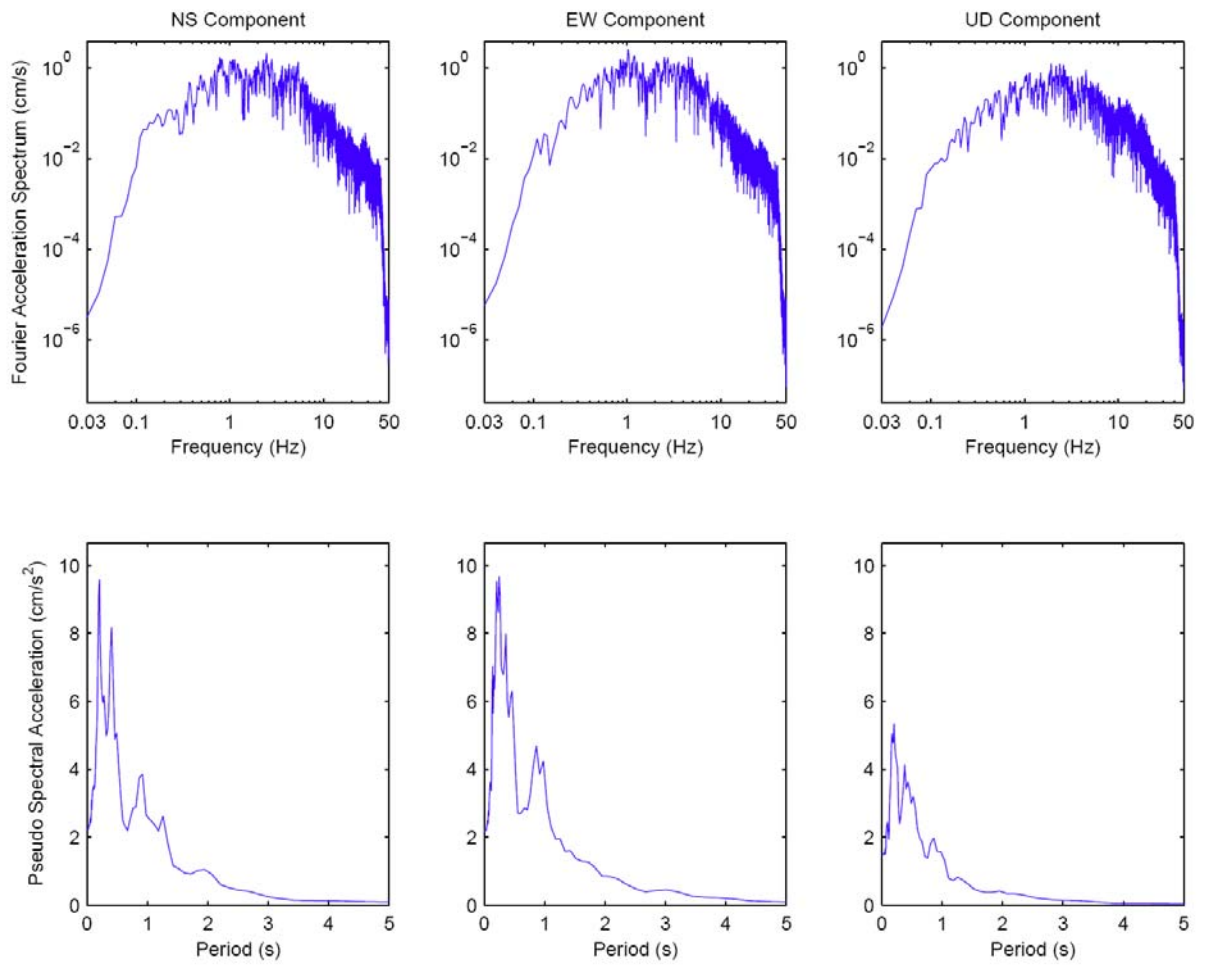
Figure 33. Fourier acceleration spectra (top row) and 5-percent damped pseudo-spectral accelerations (bottom row) of the processed ground motions recorded at Bingöl-Merkez (Record Name: 20100308101423_1201, Station Code: 1201).

Figure 34. Acceleration (top row), velocity (middle row) and displacement (bottom row) time series of the processed ground motions recorded at Bingöl-Karlıova (Record Name: 20100308101423_1206, Station Code: 1206). The waveforms are band-pass filtered by acausal 4-pole/4-pole Butterworth filter. Zero pads due to acausal filter transients are not shown for illustrative purposes.

Figure 35. Fourier acceleration spectra (top row) and 5-percent damped pseudo-spectral accelerations (bottom row) of the processed ground motions recorded at Bingöl-Karlıova (Record Name: 20100308101423_1206, Station Code: 1206).
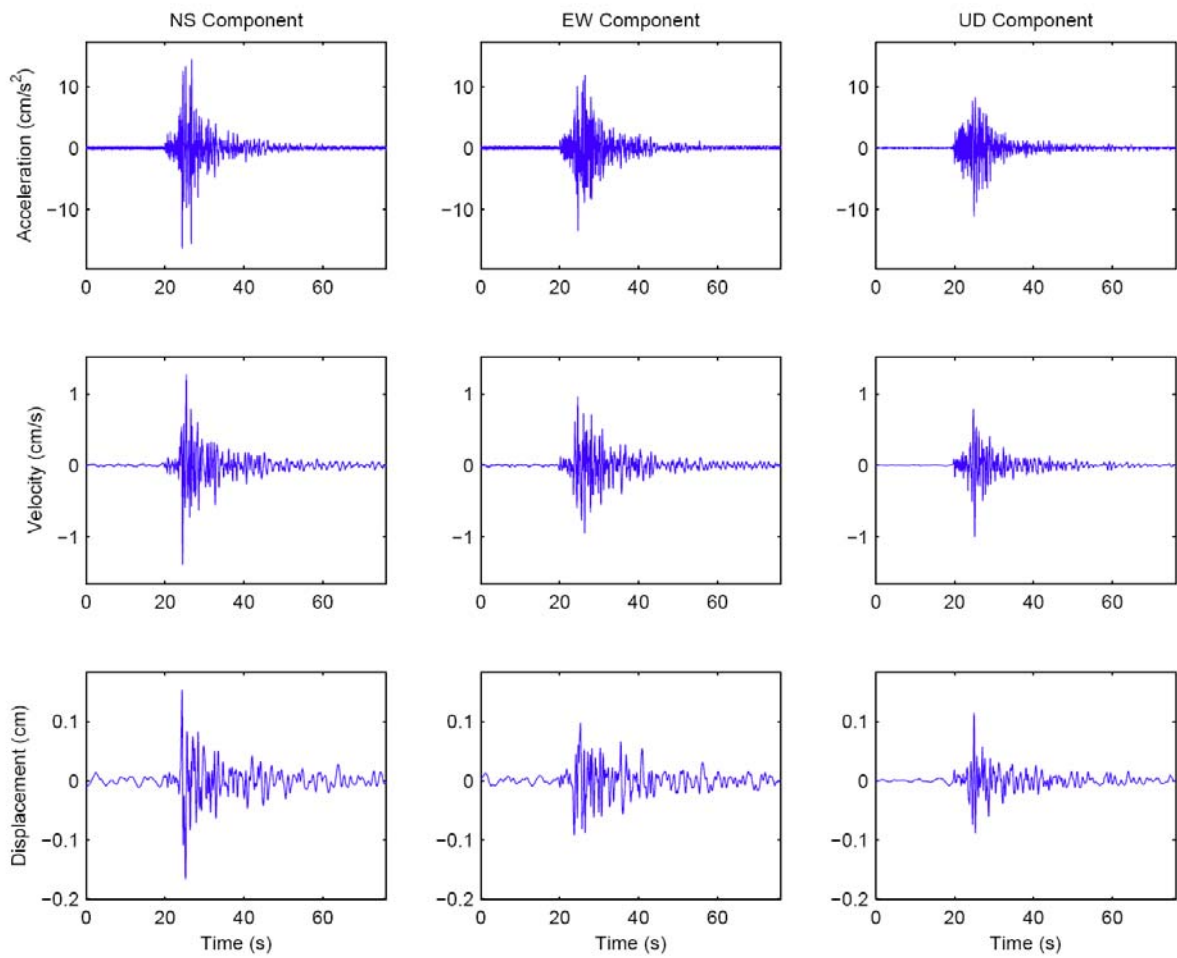
Figure 36. Acceleration (top row), velocity (middle row) and displacement (bottom row) time series of the processed ground motions recorded at Elazığ-Palu (Record Name: 20100308101423_2303, Station Code: 2303). The waveforms are band-pass filtered by acausal 4-pole/4-pole Butterworth filter. Zero pads due to acausal filter transients are not shown for illustrative purposes.
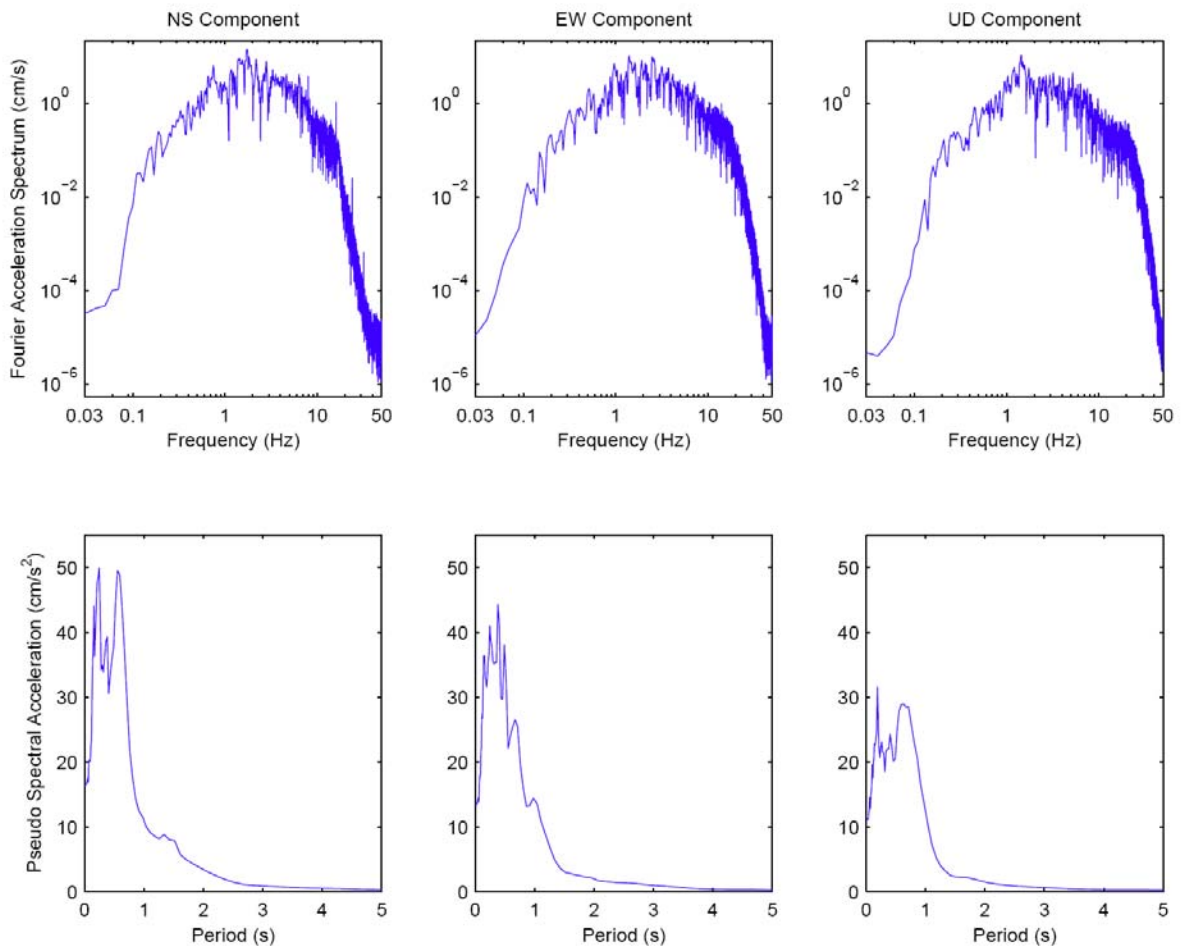
Figure 37. Fourier acceleration spectra (top row) and 5-percent damped pseudo-spectral accelerations (bottom row) of the processed ground motions recorded at Elazığ-Palu (Record Name: 20100308101423_2303, Station Code: 2303).

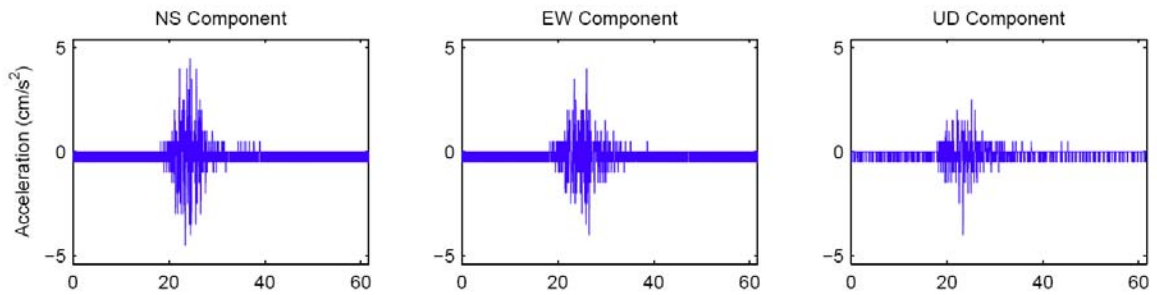**Ground Motions with Insufficient Digitizer Resolution (IDR) Problem**



Figure 37. Unprocessed acceleration time series of the ground motions recorded at Elazığ-Palu (Record Name: 20100308032022_2303, Station Code: 2303).
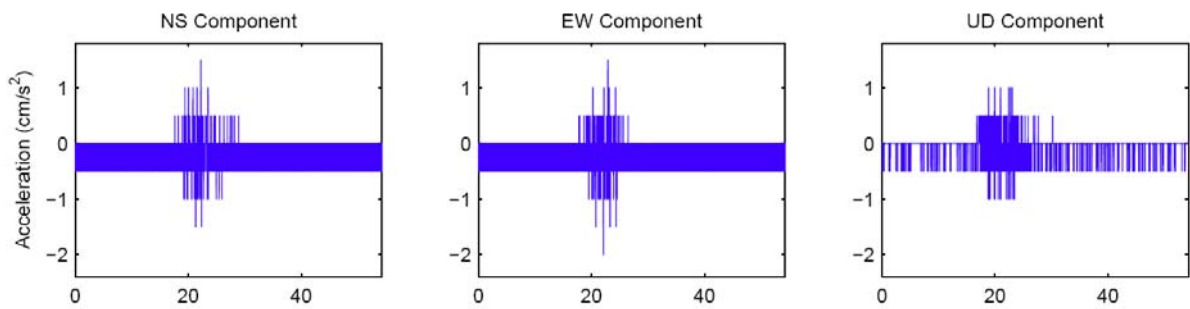


Figure 38. Unprocessed acceleration time series of the ground motions recorded at Elazığ-Palu (Record Name: 20100308XXXXXX_2303, Station Code: 2303).